METHOD FOR DETERMINATION OF SINGLET OXYGEN QUANTUM YIELDS FOR NEW FLUORENE-BASED PHOTOSENSITIZERS IN AQUEOUS MEDIA FOR THE ADVANCEMENT OF PHOTODYNAMIC THERAPY

by

WADE GRABOW
B.S. Chemistry, United States Air Force Academy, 2001

A thesis submitted in partial fulfillment of the requirements
for the degree of Master of Science
in the Department of Chemistry
in the College of Arts and Sciences
at the University of Central Florida
Orlando, Florida

Spring Term
2004

ABSTRACT

Photodynamic therapy (PDT) has been investigated over the past three decades and is currently an approved therapeutic modality for skin cancer, the treatment of superficial bladder, early lung and advanced esophageal cancers, and age-related macular degeneration in a number of countries. In PDT, the absorption of light by a chromophore generates cytotoxic species such as reactive singlet oxygen, leading to irreversible destruction of the treated tissue. The measurement of the singlet oxygen quantum yield (ϕ_Δ) is an important determinant used to evaluate the efficiency of new photodynamic therapy agents developed in the laboratory, to screen potential photosensitizers in aqueous media.

The singlet oxygen quantum yield is a quantitative measurement of the efficiency in which photosensitizers are able to use energy, in the form of light, to convert oxygen in the ground state to the reactive species singlet oxygen, $O_2(^1\Delta_g)$, useful in photodynamic therapy. Singlet oxygen quantum yields of photosensitizers differ when measured in different solvents. The majority of the existing ϕ_Δ values found in literature for various photosensitizers are documented with the sensitizers in organic solvents though values in aqueous media are more valuable for actual applications. Determination of accurate and precise ϕ_Δ values in aqueous solution is a much more difficult problem than in organic media. Problems in aqueous solution arise primarily from the physicochemical properties of $O_2(^1\Delta_g)$ in water. Singlet oxygen has a

much shorter lifetime in water than it does in organic solvents, causing challenges with respect to quantitative detection of $O_2(^1\Delta_g)$.

The ensuing pages are an attempt to explore the theory and document the procedures developed to provide the accurate measurement of $O_2(^1\Delta_g)$ in aqueous media. Details of this experimental method and singlet oxygen quantum yield results of new compounds relative to established photosensitizers will be presented.

I dedicate this work to my beautiful and amazing wife Amy. None of this would have ever been possible without her understanding, patience, and encouragement. I thank God for this opportunity and experience, to include all that I have learned about myself and what is really important in life as a result of these last two years of determined work.

ACKNOWLEDGMENTS

This thesis would not have been possible without the help of a number of individuals. I would like to thank Dr. Kevin Belfield and his research group for all of the support that they provided throughout the last two years. Particularly, I would like to thank Katherine Schafer for all the times she went out of her way to help me. Lastly, I would like to thank my friends and family who helped me along the way. Thank you.

TABLE OF CONTENTS

LIST OF FIGURES

LIST OF TABLES

LIST OF ABBREVIATIONS

PS	Photosensitizer
ϕ_Δ	Singlet oxygen quantum yield
ν	Wavenumber
τ_T	Triplet state lifetime
λ_{max}	wavelength of maximum absorption
A	Singlet oxygen acceptor
$^1O_2$	Singlet oxygen
FFA	Furfuryl alcohol
RB	Rose Bengal
PDT	Photodynamic therapy
HpD	Hematoporphirin Derivative
LED	Light Emitting Diode
DPBF	1,3-diphenylisobenzofuran
h	Planck's constant
c	speed of light
isc	intersystem crossing
NIR	Near Infrared

TRTL Time-resolved thermal lensing

LIOC Laser induced optical calorimetry

INTRODUCTION

The expression "photodynamic effect" was first contrived a century ago in 1904 by H. von Tappeiner, in an attempt to describe the fluorescence in protozoa after the application of aniline dyes.[1,2] Not only did the experiment prove to be toxic to cells, inspiring its application in tissue destruction, but it was also noted to consume oxygen in the process. Nearly six decades would pass before Richard Lipson would discover, in the 1960s, that photosensitizers possessed the ability to photodynamically destroy cells.[3] As the potential for photodynamic therapy (PDT) of tumors has grown and been proven, a steady increase in this area of study continues to occur. The basic function and application of PDT are forthright (Figure 1). The goal of PDT consists of inducing efficient photosensitized necrosis of the tumor without detriment to the surrounding healthy tissue.[4-10] The photosensitizer formulation is typically administered intravenously or, in some instances, topically.[2,11] The sensitizing drug is allowed to preferentially accumulate in the tumor. A deliberate amount of light at the appropriate wavelength is delivered to the diseased tissue causing the generation of a cytotoxic species, singlet oxygen, $O_2(^1\Delta_g)$, being the most predominant reactive and prevalent, which then kills the surrounding tumor or diseased cells.

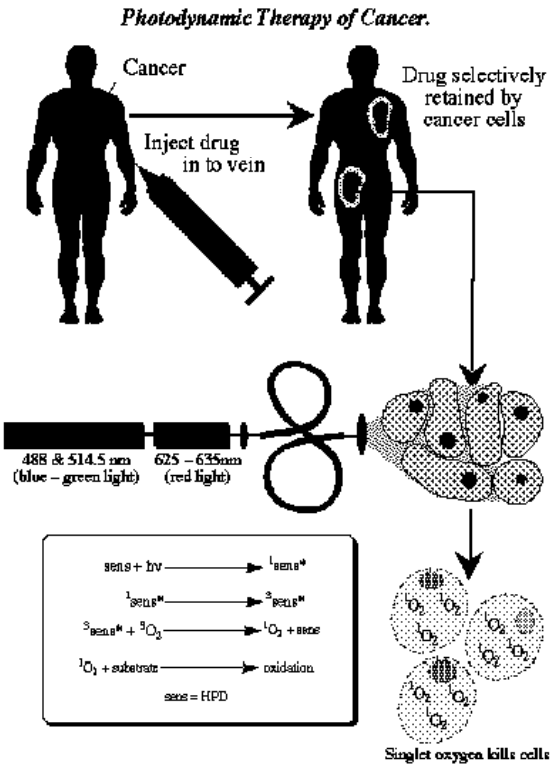

Figure 1. Overview of PDT

The most common way in which singlet oxygen is generated is by electronic excitation transfer from appropriate photosensitizers, as is the case in photodynamic therapy. The general process follows:

$$\text{Sensitizer } (S_0) \xrightarrow{h\nu} \text{Sensitizer}^{*}(S_1) \xrightarrow{\text{isc}} \text{Sensitizer } (T_1) \qquad (1)$$

$$\text{Sensitizer } (T_1) + {}^3O_2 \longrightarrow \text{Sensitizer } (S_0) + {}^1O_2 \qquad (2)$$

Equation 2 is valid because the net change in spin before and after the reaction remains unchanged (Figure 2).[5]

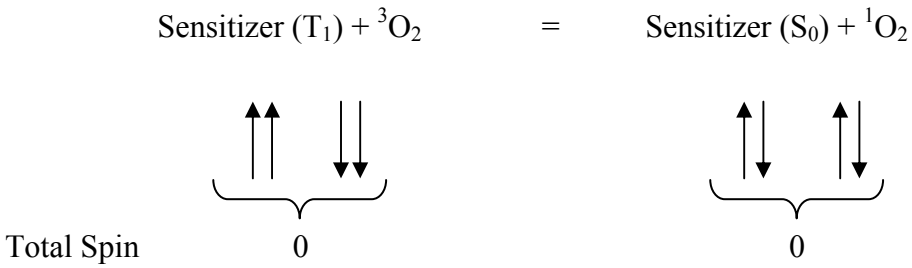

Figure 2. Spin conversion

One of the goals of PDT research is to make sensitizers that are able to follow this process of converting ground state oxygen to singlet oxygen as efficiently as possible. The singlet oxygen quantum yield is a measure of the efficiency of this overall process. The desired outcome is singlet oxygen because it is the ultimate reactive species, which induces irreversible destruction of cells within the irradiated tumor area.[2,3,9-12] It goes almost without saying that the ϕ_Δ must be less than ϕ_T, where ϕ_T is the quantum yield or efficiency of a sensitizer to go from its ground state to the excited triplet state upon irradiation.[5]

Although, photodynamic therapy has been employed against a number of different cancers including bladder, brain, breast, skin, colorectal, head, neck, and oral types of cancer only a few drugs have been approved for such treatments.[6-10] Currently Photofrin II®, a purified hematoporphyrin derivative (HpD), is the only PDT drug approved by the US Food and Drug Administration.[7-10] The first generation photosensitizers like Photofrin I® and Photofrin II® suffer from a number of drawbacks causing limited acceptance and applications. Such first

generation photosensitizers consist of a mixture of several uncharacterized porphyrins that lack selectivity for cancer cells. Their low extinction coefficients mandate the use of large doses of the drug in order to achieve sufficient phototherapeutic gains. The first generation photosensitizers typically hold absorption maximum around 630 nm, prohibiting appreciable tissue penetration.[2,4] Lastly, they suffer from prolonged generalized skin photosensitivity, lasting up to 6-8 weeks, confining their use to a small number of selected patients with extensive and surgically inoperable lesions.[2,3,11,12]

Newer second-generation photosensitizers offer improvements in an attempt to address some of the shortfalls associated with the first generation photosensitizers. The class of second-generation photosensitizers consists of highly purified and characterized compounds to include: porphyrins, phthalocyanines, naphthalocyanines, bacteriochlorins, texaphyrins, and others.[4,12] These photosensitizers exhibit absorption peaks with a longer wavelength than that of the first generation. Typically their absorption maximum is in the range of 650-800 nm. This affords greater penetration of light into the irradiated tissue. The second-generation photosensitizers are also designed to be more selective, preferring to accumulate in cancerous tissue as opposed to healthy tissue. A major problem still remains. Most of these photosensitizers are hydrophobic and they therefore are not conducive to intravenous applications. A significant amount of research is currently being dedicated to the study of potential delivery systems to overcome a photosensitizer's hydrophobic construct, facilitating passage through the predominately aqueous bloodstream.[10-12]

As previously stated, the singlet oxygen quantum yield (ϕ_Δ) is a term used to describe the

measurement relating to the efficiency in which photosensitizers are able to absorb light and convert oxygen in the ground state to an excited singlet state referred to as singlet oxygen. Traditionally the absorption of light has involved that of a single photon at a specific energy or wavelength necessary to excite the sensitizer from its ground state to its first excited state. A new process involving "two-photon absorption" has been gaining interest and popularity over the past few years.

Two-photon absorption and sensitization are being investigated in an attempt to overcome existing limitations encountered in photodynamic therapy and the second-generation photosensitizers. Two-photon absorption is non-linear optical process. In two-photon absorption and excitation, sensitizers exposed to high intensity light can experience simultaneous absorption of two lower energy (longer wavelength) photons, which, together, synergistically provide the energy necessary to cause excitation of the sensitizer.[13,14] The theory behind and advantages of two-photon absorption will be explored further in the next section.

BACKGROUND

Cancer is currently the second leading cause of death in the United States and Western Europe behind heart disease. Cancer is often described as an uncontrollable rapid proliferation of cells, which typically spread throughout the local tissues and body disrupting adjacent cells in the process, giving rise to metastases. The main goal in cancer therapy involves destroying the cancerous cells while preserving the healthy cells. This selectivity is often compromised by toxicity of the treatment. Often times, the treatment is too effective in that it cannot adequately discriminate between the two types of cells present, i.e. cancerous or healthy.

Significant progress has been made in treatment of different types of cancer in the past few decades. Advancements in chemotherapy, the use of drugs acting systemically to cure cancer, in combination with radiotherapy and surgery have led to higher success rates in the treatment of testicular cancer, Hodgkin's lymphoma, and others.[2] Such therapies rely on the synergistic effects created with a combination of treatments that are used to essentially wear down the cancer cells over time. Although advancements in cancer treatment in current times continue much work still remains to be done. Photodynamic therapy is a promising treatment for a variety of oncological, cardiovascular, dermatological, and ophthalmic diseases due to its potential for extraordinary selectivity toward cancerous cells exclusively.[2]

The first and most pronounced level of selectivity comes from the inherent mechanism of

the photosensitizer. Ideally the sensitizer remains biologically inactive within the body until it is photoactivated by the irradiation of light. The second level of selectivity comes from designing the sensitizer so that it can preferentially accumulate in tumors rather than normal cells. This affect can be achieved by binding photosensitizers to molecular delivery systems that have high affinity for the target tissue.[9-11,15] The majority of the current sensitizers are predominately hydrophobic in nature making them lipophilic. The realization that tumor selectivity increases with the lipophilic character of the sensitizer is well demonstrated and accepted.[6,8] This realization does not occur without its consequences. The lipophilic nature of current sensitizers, while being important with respect to preferentially accumulation and selectivity toward tumors, makes them less water-soluble and therefore intravenous treatment becomes much more difficult. Different strategies to deliver the sensitizer to the diseased tissues are being evaluated, including the use of liposomes, oil-dispersions, polymeric particles, hydrophilic polymer-PS conjugates, and using the target tissue receptors or antigens.[2] In theory, any increase in selectivity due to these accumulation strategies will ultimately be compounded by the inherent selectivity of the overall therapy and could lead to unprecedented degrees of discrimination for the destruction of diseased cells leaving the healthy cells unaffected.

Although photodynamic therapy relies on the involvement of three different components: photosensitizer, light, and molecular oxygen, the photosensitizer remains the most important component because it dictates the wavelength of light that can be used and it is responsible for the efficiency in which ground state oxygen can be converted to singlet oxygen. It must be noted though that other two components remain essential because without any one of these three

components the desired biological effect in the system will not occur.[2,,4,11,12,15] The relationship between these three components, and their codependency for successful and efficient PDT, makes for an extremely fascinating and adaptable application in cancer therapy.

Photofrin, a purified haematoporphyrin derivative, was the first photosensitizer to receive regulatory approval and is currently the most common drug in use as a therapeutic sensitizer with respect to PDT.[6,8] The second most widely clinically employed sensitizer is haematoporphyrin derivative (HpD), which consists of a number of different porphyrin derivatives in varying forms.[16] Unfortunately, this class of first-generation sensitizers is known to suffer from a number of significant drawbacks. Photofrin and other porphyrin derivatives lack chemical homogeneity and stability. They are known to cause long-term skin photosensitivity in patients and they have unfavorable physiochemical properties and low selectivity with regard to uptake and retention by diseased cells with respect to normal cells. Additionally, they have relatively weak absorption in the 700-900 nm spectral window where optimal penetration of light into tissue occurs.[6,8]

A significant effort in relation to PDT is being focused on the development of new sensitizers known as second-generation photosensitizers. These new compounds are being developed to replace and ultimately solve some the problems associated with the first generation sensitizers. These second generation sensitizers, including phthalocyanines, naphthalocyanines, chlorins, bacteriochlorins, purpruins, and tetrabenzoporphyrins, have shown an increased photodynamic efficiency in the treatment of animal tumors, absorption at longer wavelengths, and reduced phototoxic side effects.[17]

Although typically the most important factor to consider when assessing a potential sensitizer for use in PDT is the singlet oxygen quantum yield; it is not the only parameter that should be taken into account when considering potential candidates. A compound can have a ϕ_Δ of one but remain useless if it is found to be toxic to humans at clinical doses prior to activation. There are a number of other parameters that must also be considered. Biologically, potential photosensitizers should be nontoxic to normal tissues at the doses necessary for PDT and should preferentially accumulate around and within tumors and diseased tissues.[6,9,18,19] Chemically, sensitizers should have a relatively long half-life in the dark in serum and tissues undergoing PDT. Additionally they must be sufficiently soluble in water while at the same time maintaining a hydrophobic character allowing for accumulation in tumor tissues. Spectroscopically, they should possess strong absorption bands at long wavelengths, at which there is no interference from other chromophores that exist in tissues. Thus, light penetration into the tissue is enhanced. Quantum mechanically, candidate sensitizers should be able to undergo the process of intersystem crossing efficiently, and maintain a sufficiently long triplet state lifetime (τ_T)[3]

After all of these considerations are taken into account, the photosensitizer must still be able to undergo one of two known processes by which light, in the presence of a photosensitizer and dioxygen, promote a chemical reaction to produce the desired cytotoxic agent used in photodynamic therapy. The two broad mechanistic categories in which the cytotoxic agent is produced are referred to as Type I and Type II mechanisms respectively.[18]

The Type I process is characterized by the absorption of a photon by the sensitizer, elevating it to from the ground state to the excited state. This excited state generates either a

radical species by hydrogen atom abstraction from a substrate (scheme a) or superoxide radical anion via electron transfer (schemes b and c).[5] The radical species then reacts with ground state oxygen so that the overall reaction is a photochemically initiated autoxidation to generate the cytotoxic agent depicted by the following set of chemical equations:

a) $\text{Sensitizer } (S_0) \xrightarrow{h\nu} \text{Sensitizer } (S_*)$ (3)

$\text{Sensitizer } (S_*) + A \xrightarrow{e \text{ transfer}} \text{Sensitizer } (S^{\cdot+}) + A^{\cdot-}$ (4)

$\text{Sensitizer } (S_*) + AH_2 \xrightarrow{H \text{ atom transfer}} \text{SensitizerH } (SH^{\cdot}) + (AH)^{\cdot}$ (5)

$(AH)^{\cdot} + {}^3O_2 \longrightarrow AH\text{-}OO^{\cdot} \longrightarrow \text{Products}$ (6)

b) $\text{Sensitizer } (S_0) \xrightarrow{h\nu} \text{Sensitizer } (S_*)$ (7)

$\text{Sensitizer } (S_*) + {}^3O_2 \xrightarrow{e \text{ transfer}} \text{Sensitizer } (S^{\cdot+}) + O_2^{\cdot-}$ (8)

superoxide

c) $\text{Sensitizer } (T_1) + A \longrightarrow \text{Sensitizer } (S^{\cdot-}) + A^{\cdot+}$ (9)

$$\text{Sensitizer } (S^{\bullet-}) + {}^3O_2 \xrightarrow{e\ transfer} \text{Sensitizer } (S_0) + O_2^{\bullet-} \qquad (10)$$

superoxide

The Type II process is the process responsible for the generation of singlet oxygen, the predominant cytotoxic species generated and employed in photodynamic therapy. In the Type II process, oxygen reacts with an excited state of the sensitizer by energy transfer (via triplet-triplet interactions) to form the reactive species singlet oxygen.[5,18] The overall process of generating singlet oxygen is represented by the following set of equations:

$$\text{Sensitizer } (S_0) \xrightarrow{h\nu} \text{Sensitizer } (S_1) \xrightarrow{\text{isc}} \text{Sensitizer } (T_1) \qquad (11)$$

$$\text{Sensitizer } (T_1) + {}^3O_2 \longrightarrow \text{Sensitizer } (S_0) + {}^1O_2 \qquad (12)$$

$$\text{Biomolecule} + {}^1O_2 \longrightarrow \text{products} \qquad (13)$$

The sensitizer is activated by the absorption of light and is excited from the ground state to the first excited singlet-state. It can then relax back to the ground state by fluorescing and emitting a photon or can transition to an excited triplet state via intersystem crossing (ISC). The sensitizer in the excited triplet state can then either relax back to the ground state by phosphorescing and emitting a photon or by transferring energy to oxygen via radiationless

transition converting the ground state triplet oxygen to singlet oxygen.

Light, as revealed by the mechanism of singlet oxygen generation, is the second ingredient required to elicit the photodynamic effect used in photodynamic therapy. The definition of PDT is typically constrained to the "use of visible or near infrared light" consisting of localized delivery to tumors (Figure 3).[5,20] Visible light is located between ultraviolet light and infrared energy in the electromagnetic spectrum shown in figure 3.

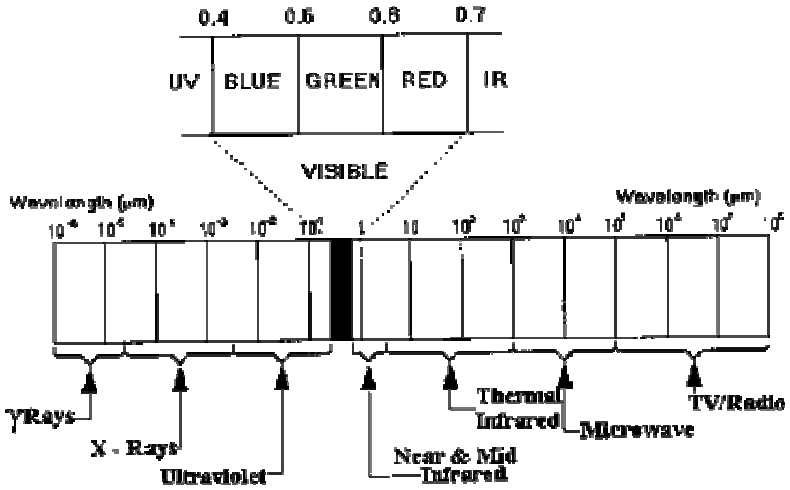

Figure 3. Electromagnetic spectrum

A variety of light sources have been used for activation of a number of sensitizers in PDT, including argon, solid state, and diode lasers, as well as tungsten filament quartz halogen, xenon arc, metal halide, and fluorescent lamps. Further development of photonic technology has brought about the use of light emitting diodes (LED) coupled with fiber-optic waveguides, allowing for potential use of PDT within the body, overcoming some of the shortfalls found with limited penetration of other light sources.[20,21] Lasers remain to be the most frequently used light

sources because they produce highly coherent monochromatic light that can be efficiently channeled into quartz fibers used as light delivery devices. Laser technology is advancing in such a way that they are becoming more portable, tunable, reliable, and cheaper each passing day.

Efficient PDT depends upon penetration of light into only the area involving the infected tissue. The depth of penetration of light in the tissue is directly related to the appropriate wavelength in which illumination of the chromophore takes place.[3] Light with a wavelength near 800 nm is known to penetrate through human tissue deeper than at shorter wavelengths. Figure 4 illustrates how transmittance properties of a tissue change with respect to the wavelength of the light used. The figure also shows the absorption spectra relating to some of newer generation photosensitizers. One of the goals involving the development of new sensitizers is designing them so that they are able to take advantage of the tissue transmission window found near 800 nm.[7,8,10]

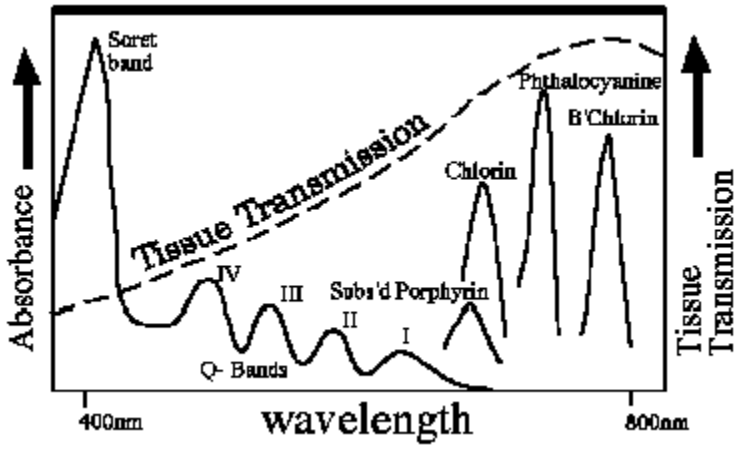

Figure 4. Tissue transmission and absorption ranges of 2nd generation sensitizers

The potential of using longer wavelengths of light for applications involving two-photon photodynamic therapy offers the possibility of many benefits toward the application of light. Although the mechanism and selection rules of excited-state population differ between one- and two-photon absorption, the overall outcome resulting in the creation of the lowest excited singlet-state, S_1, via internal the sensitizer remains the same.[5,13] As the name implies, the two-photon absorption process involved in PDT entails the simultaneous absorption of two photons, either degenerate or non-degenerate, at wavelengths much longer than the linear absorption spectrum of the particular sensitizer by the means of a "virtual state" nominally residing in the region somewhere between the ground and excited state.[14,22-24]

The strength of the two-photon absorption effect lies in the fact that such absorption depends on the intensity of the light squared.[24-26] This characteristic intensity-dependence of absorption means that the laser light is only strongly absorbed at the focus of the microscope objective lens. This characteristic increases the selectivity of PDT because it decreases the amount of scattering or diffusion of light that occurs at the edges of the light beam. Additionally, two-photon absorption allows for the use of sensitizers that normally absorb in the ultra-violet (UV) region of the electromagnetic spectrum. In general, a sensitizer that normally absorbs light at a higher energy (400 nm) can be excited with the use of light at a lower energy (800 nm) if two-photon absorption is employed. The use of a longer wavelength of light, as previously stated, increases the penetration depth into the tissue as shown in Figure 5.

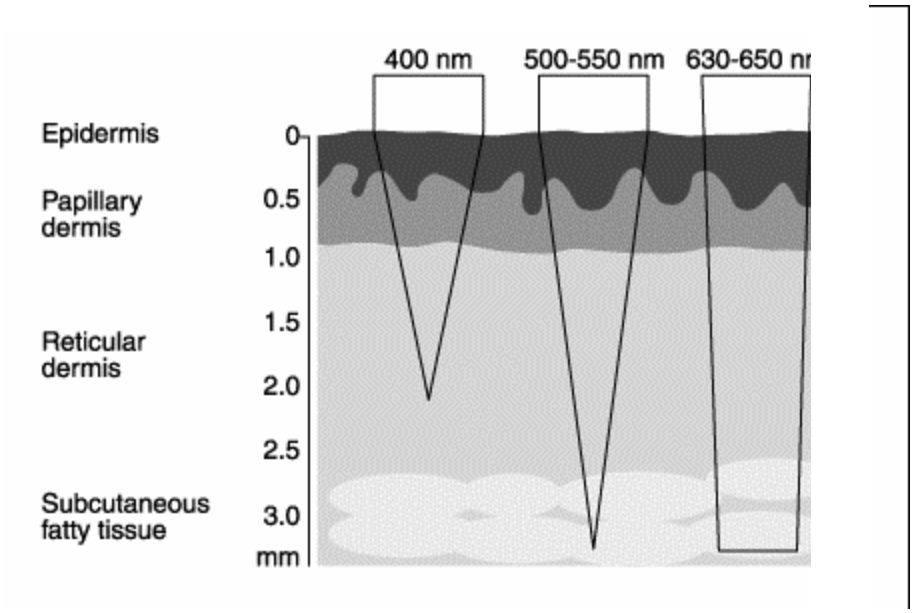

Figure 5. Tissue penetration with respect to wavelength[28]

Oxygen, specifically singlet oxygen, is the final key component, integral to the application of photodynamic cancer therapy. As previously stated, singlet oxygen is generated by a Type II reaction.[2,3,27] Prior to this reaction, however certain criteria must be met and certain occurrences must take place. A Jablonski diagram is commonly used to explain such phenomena (Figure 6).

Photodynamic therapy begins with the absorption of a photon by the photosensitizer. The upward blue arrow represents this occurrence and letter "A" illustrated in the following diagram labeled figure x. Absorption of the photon elevates an electron from the ground state to an excited state, shown here as S_2. The electron then typically undergoes a transition to occupy the lowest excited state through an internal conversion process. The electron at this point can either lose energy by relaxing back to the ground state and emit light, denoted on the diagram as the

green downward arrow and the letter "F", or undergo an intersystem crossing phenomenon and occupy an excited triplet state.[5] Once again, one of two things can happen with respect to the electron. It can either relax back to the ground-state, emitting a photon, as in the case of phosphorescence denoted by the downward pointing red arrow and the letter "P", or it can undergo an internal conversion process and occupy the lowest available triplet-state. If the latter process occurs, then the system is available for the generation of singlet oxygen via the Type II process involving a spin coupling interaction with oxygen in its triplet ground-state.[5,18]

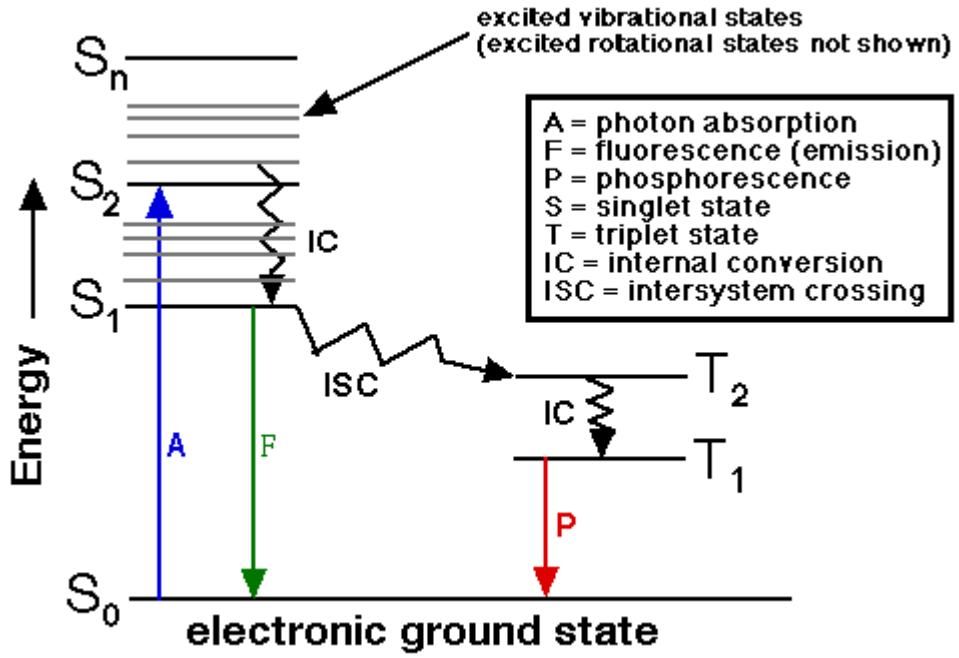

Figure 6. Jablonski diagram

The amount and efficiency in which singlet oxygen can be generated by a particular

photosensitizer is often considered to be the most important parameter to consider when assessing candidate sensitizers. This efficiency is known as their singlet oxygen quantum yield. The ϕ_Δ is typically described as the number of molecules of singlet oxygen generated per number of photons absorbed by the sensitizer. Because the absorption of a single photon has the capacity to generate only one molecule of singlet oxygen in an ideal situation, the ϕ_Δ of a sensitizer is an integer with a value between zero and one. A ϕ_Δ of one would correspond to the perfect sensitizer in which every single photon absorbed correlates to the generation of a singlet oxygen molecule. A number of different techniques for the determination of this measurement of efficiency have been developed, tested, and used over the past four to five decades. Various methods for accurate determination of singlet oxygen quantum yields include direct methods, in the case of time-resolved near-infrared (NIR) luminescence, time-resolved thermal lensing (TRTL), and laser-induced optoacoustic calorimetry (LIOAC).[28-31] The NIR luminescence technique is considered to be a direct method because the very weak emission of $^1O_2$ in the NIR, around 1290 nm, is monitored directly.[29,30] The two most prevalent indirect methods include chemical trapping and O_2 consumption methods. Among the different methods involving chemical trapping, numerous types of traps and modes of monitoring exist. Depending upon the trapping species, chemical traps can be monitored by changes in fluorescence, EPR, absorption, and others.[19,27,32-34]

Methods involving chemical trapping are typically more widespread, due to the fact that they do not typically require the amount of specialized and expensive equipment, as other methods like the NIR luminescence technique does. They are also typically the most

straightforward and understood method, suitable for routine laboratory applications because an extensive amount of work pertaining to the mechanism of singlet oxygen and its acceptors are now well documented in literature.[42,43,47,48,52] Additionally, chemical trapping methods have been found to be better suited for use in both organic and aqueous media.

One of the important characteristics of a sensitizer relates to its degree of hydrophilicity. More hydrophobic compounds are known to preferentially accumulate in tumor and denser tissue infected by cancer. Because of this known phenomenon, predominately hydrophobic sensitizers have been at the forethought of development. Subsequently the first studies aimed at doing ϕ_Δ measurements have been almost exclusively conducted in the presence of different types of organic solvents because potential sensitizers have been significantly more soluble in organic solvents that that of water.

A significant amount of data covering many various sensitizers and substrate molecules have allowed a number of conclusions to be drawn concerning, among other things, singlet oxygen's lifetime dependency on the particular solvent environment present.[35-39] Table 1 shows the relative lifetime of $^1O_2$ in the presence of different solvents.[38,40]

Table 1. Lifetime of singlet oxygen as a function of solvent

Solvent	$^1O_2$ lifetime (μs)
Water	2
Deuterated water	68
Methanol	7
Ethanol	11
Hexane	24
Chloroform	247
Carbon tetrachloride	59000

The singlet oxygen quantum yields of numerous organic photosensitizers are well documented in a variety of organic solvents. The singlet oxygen quantum yield for a particular sensitizer is found to vary between different solvents. Difficulties have primarily been encountered with respect to measurements of singlet oxygen quantum yield in aqueous media. The problems arise from aggregation of the sensitizer, pH and/or ionic strength effects, competitive formation of superoxide ions, and the physicochemical properties of singlet oxygen in water, primarily the short lifetime of singlet oxygen in aqueous media.[38,41] Such problems have made accurate singlet oxygen quantum yield determinations difficult, with poor agreement between literature values. Literature values for the photosensitizer hematoporphyrin range from 0.74 to 0.12.[41]

This dependency of the lifetime of $^1O_2$ in different solvents, particularly in water causes added difficulty when attempting to accurately determine the efficiency of varying sensitizers. Although monitoring $^1O_2$ with the use NIR luminescence could potentially be considered the most accurate method because it is a direct method, it has not found wide spread use. The fact that the equipment necessary to employ such a method is expensive pertains to part of the reason. The other reason is that the intensity of the $^1O_2$ emission is extremely weak in water.[27,42] Because the lifetime of $^1O_2$ is so much shorter in water when compared to other solvents, the probability of emission is much lower causing the lower emission intensity.[27] Subsequently, early NIR detection systems have not been sensitive enough for use in aqueous media other than in D_2O, where the singlet oxygen lifetime is known to be significantly increased. The one significant drawback of direct detection is that it requires the use of a highly sensitive IR detectors and equipment.[29,30,43]

Similar problems hold true for two of the other direct methods used to measure the singlet oxygen quantum yield of different sensitizers. Unlike the luminescence techique that monitors the radiative decay of $^1O_2$, the LIOAC and TRTL techniques follow the non-radiative relaxation of excited species. These methods also suffer in aqueous media, owning to the fact that sensitivity of these techniques are once again highly solvent dependent. Water possess the unfavorable physical properties of having a high specific heat capacity, a low thermal expansion coefficient, and a low change in refractive index with respect to temperature changes.[19] All of these factors reduce the sensitivity of these methods in water, necessitating the use of higher laser excitation energies, which are close to, or outside, the important limit of linear dependence

of signal on laser energy. As one moves away from this linear dependence the possibility of erroneous results increases. Indirect methods in contrast include the presence of a singlet oxygen acceptor compound, and monitoring either its disappearance or the appearance of its product with singlet oxygen.

The indirect methods based on the using $^1O_2$ chemical traps or following $^1O_2$ as a result of oxygen consumption have found increased utility for determining the efficiency of various sensitizers in aqueous media in recent years.[33,44-46] This is more than a trivial consideration, necessary when bearing in mind the predominantly aqueous nature of living organisms. The fact that ultimate goal is to develop a senstizer that will be used in aqueous environments (the human body) is an important point, making it crucial to study the photosensitization properties of water soluble compounds in aqueous environments.

A number of $^1O_2$ chemical traps have been investigated for use in singlet oxygen studies. One of the most well known is compound **1**, 1,3-diphenylisobenzofuran (DPBF). Its sensitized oxygenation forms *o*-dibenzoylbenzene through a [4 + 2] cycloaddition of $^1O_2$.[47-50] The disappearance of DPBF and the formation of the product *o*-dibenzoylbenzene can be monitored by absorption or fluorescence spectroscopically.

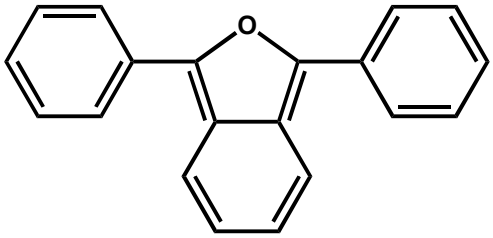

1

DPBF was used in a method described previously to determine the singlet oxygen quantum yields of different sensitizers in various organic solvents.[51] It is a good acceptor because it reacts rapidly with $^1O_2$, it does not react with the ground state (triplet) molecular oxygen nor with the superoxide anion, and its only reaction with $^1O_2$ is a chemical one.[48] The ϕ_Δ of compound **3** was determined by this method in ethanol.

Although DPBF is arguably the most well known $^1O_2$ acceptor, it is not suitable for measurements made in aqueous media.[27,52] DPBF is insoluble in water and it tends to dimerize and become unreactive toward singlet oxygen in H_2O-rich mixtures.[39] Subsequently an aqeous $^1O_2$ acceptor was needed.

A few of the known $^1O_2$ acceptors that have been used in aqueous media include: histidine, tryptophan, *p*-nitrosodimehylaniline (RNO), anthracene derivatives, and furfuryl alcohol.[27,43,46,48,52-55] The the main drawbacks relating to some of the water-soluble $^1O_2$ acceptors involve compounds with absorption in the visible light regions and/or low specificity for and reactivity with $^1O_2$. The oxygen acceptor or trap must be highly reactive and specific towards $^1O_2$. It must also be compatible with aqueous media and not interact with the photosensitizer or system being studied.[43] The spectral properties of the oxygen acceptor are also of importance. It must be transparent in the spectral range of the incident light in order to avoid photosensitization itself.

Furfuryl alcohol, compound **2**, (FFA) is a well documented singlet oxygen acceptor and does not possess the drawbacks previously listed.[27,33,46,55] FFA, as a $^1O_2$ acceptor, possesses a number of benefits. FFA has an absorption maximum λ_{max} around 215nm. This allows

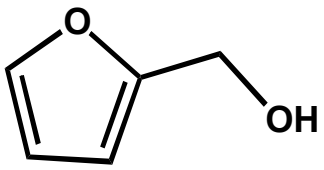

2

for no interference while exciting the sensitizer above approximately 230 nm. FFA is also known to be extremely reactive towards singlet oxygen while also being adequately specific for singlet oxygen. It is soluble and stable in aqueous solutions at a wide concentration range. In addition to being highly reactive and specific for $^1O_2$, FFA is not known to interfere with sensitizers in the ground or excited states. One possible drawback to using FFA as an $^1O_2$ acceptor is that it is known to react with $^1O_2$ to produce a mixture of oxidation products, shown in Figure 7, whose nature and relative yields vary with respect to the solvent system.[56,57] This phenomenon had no affect on the method used, because the method employed did not monitor either the disappearance of FFA or the appearance of the products. Subsequently, FFA was chosen as the singlet oxygen acceptor for use in the oxygen consumption method.

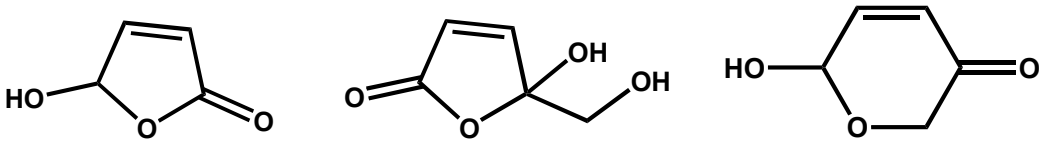

Figure 7. Products from reaction of singlet oxygen and FFA

The method employed to measure the singlet oxygen quantum yields was an indirect method using an $^1O_2$ acceptor to enable the determination of the amount of oxygen consumed. The oxygen consumption method involves measuring the oxygen concentration of the aqueous

solution of the sensitizer both prior to and after irradiation. The $^1O_2$ acceptor is used to trap the formation $^1O_2$ from $^3O_2$ and thereby create a change in the overall oxygen concentration of the system. The kinetics involved in the reaction of the $^1O_2$ in the presence of an acceptor are shown in the equations below:[45-47]

$$^1O_2 + A \xrightarrow{k_r} AO_2 \qquad (14)$$

$$^1O_2 + A \xrightarrow{k_q} {}^3O_2 + A \qquad (15)$$

$$^1O_2 \xrightarrow{k_d} {}^3O_2 \qquad (16)$$

where k_r is the rate constant of the chemical equation between the $^1O_2$ acceptor, A, and $^1O_2$ to form the trapped oxygen complex. The rate constant k_q relates to the physical quenching of singlet oxygen and the rate constant k_d relates to the natural decay of singlet oxygen to the triplet oxygen in the ground state.

The ability to monitor the production of $^1O_2$ by energy transfer from a photosensitizer (PS) is based on a chemical reaction of $^1O_2$ with a singlet oxygen acceptor (A):[45,46]

$$\Phi_{AO2} = \frac{nO_2}{n_{abs\,\lambda}} = \Phi^1O_2 \bullet \alpha \bullet \frac{k_r\,[A]}{k_d + (k_r + k_q)\,[A]} \qquad (17)$$

$$1/\Phi_{AO2} = \frac{k_r + k_q}{\alpha \bullet \Phi^1O_2 \bullet k_r} = \beta\,\frac{k_r + k_q}{\alpha \bullet \Phi^1O_2 \bullet k_r} \bullet \frac{1}{[A]} \qquad (18)$$

where Φ_{AO2} is the quantum efficiency of the photooxidation of the singlet oxygen acceptor, α is the stoichiometric factor of the chemical reaction between $^1O_2$ and FFA, and β is an acceptor specific reactivity parameter:

$$\beta = \frac{k_d}{k_r + k_q} \qquad (19)$$

As long as the rate constant of physical quenching, k_q, is insignificant compared to the rate constant of the chemical reaction, k_r, the intercept of the plot of $1/\Phi_{AO2}$ vs. $1/[A]$ is equal to $1/(\alpha*\Phi^1O_2)$. The singlet oxygen quantum yield of photooxidation of the acceptor, furfuryl alcohol, is determined by measuring the amount of oxygen consumed for different solutions with a constant sensitizer concentration and varying acceptor concentrations.

The oxygen consumption method, which has been known to be a reliable method for the determination the efficiency of singlet oxygen production of sensitizers, was used in the present work to obtain accurate values for the quantum yields.[33,45,46,55,57,58,] A known standard, rose bengal (RB), whose chemical structure is shown in below, was used to verify use of the method. In addition, the ϕ_Δ of a new water-soluble photosensitizer developed in Dr. Belfield's research group was measured.

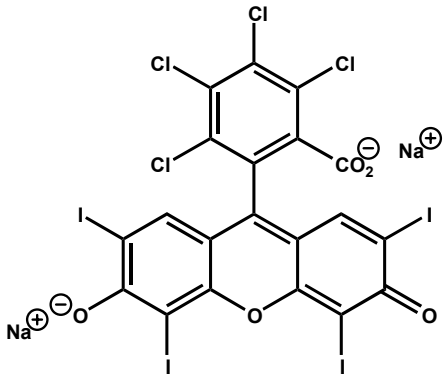

4

Oxygen consumption was measured by using an oxygen probe manufactured by Ocean Optics. The needle-tip fiber optic oxygen probe uses the fluorescence of a ruthenium complex in a sol-gel to measure the partial pressure of oxygen.[61] A blue LED sends light at ~475 nm, through an optical fiber. The fiber carries the light to the tip of the probe, which consists of a thin layer of a hydrophobic sol-gel material. The sol-gel material has an immobilized and protected ruthenium complex trapped within it. The light from the LED excites the ruthenium complex and the causes it to fluoresce at ~600 nm. The fluorescence is quenched by a non-radiative transfer of energy to oxygen molecules.[59-62] The degree of quenching correlates to the partial pressure of oxygen in the film which is directly proportional to the oxygen concentration. The ruthenium emission is carried back through the fiber optical cable to the spectrometer. An A/D converter converts the analog data to digital data that the PC relays as the arbitrary intensity, which is calibrated to give an accurate oxygen concentration.

RESEARCH OBJECTIVES

The research objectives are outlined below:

1. Research known methods for determination of singlet oxygen quantum yields in aqueous solutions.
2. Select best method for use in laboratory based on: required equipment, cost of equipment,
3. Design and develop method to measure singlet oxygen quantum yield in aqueous solution based on methods researched.
4. Prove method works.
5. Compare singlet oxygen quantum yield measurements for methods developed using DPBF and FFA as $^1O_2$ acceptors in ethanol and water respectively.

EXPERIMENTAL

Previous work by Dr. Belfield's research group focused on determining the singlet oxygen quantum yield of different sensitizers in organic solvents, primarily ethanol.[51] The technique used to determine the $\Delta\Phi$ consisted of an indirect method using DPBF as the singlet oxygen acceptor. DPBF is a fluorescent molecule and the reaction of singlet oxygen with DPBF could be monitored because the product was not fluorescent. The decline in fluorescent intensity was monitored in a spectrofluorometer. This signal could be correlated to the amount of singlet oxygen generated and could be used to determine the singlet oxygen quantum yield of a sensitizer.

It was by this method explained above that the $\Delta\Phi$ of the compound **3** was first measured in ethanol using the DPBF method previously described. Compound **3** was chosen because it possesses a λ_{max} which allows for potential two-photon excitation in the near infrared. Thus, this class of molecules may be suitable for two-photon PDT.

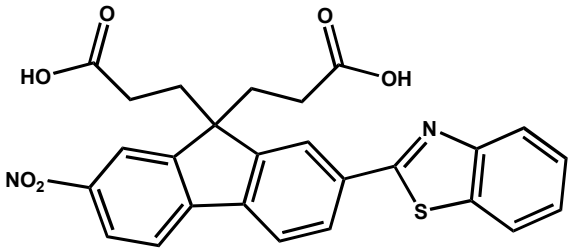

3

Experimental trial and error proved that DPBF was not a suitable $^1O_2$ acceptor in aqueous media. Literature documentation supported the experimental problems encountered using DPBF as a singlet oxygen acceptor in aqueous media. Subsequently a new method and/or $^1O_2$ acceptor was needed in order to accurately determine singlet oxygen efficiencies of water soluble sensitizers in aqueous media.

After a considerable amount of research concerning the assorted methods for accurate $\Delta\Phi$, the oxygen consumption method was chosen for the various reasons mentioned in the background section. The method was designed using the equipment set-up illustrated in Figure 8, and described below.

The oxygen consumption method is based on monitoring the decline in oxygen concentration in solution as a result of furfuryl alcohol acting as a singlet oxygen trap. The photosensitizer is irradiated with a known amount of light for a specific amount of time at the specified wavelength, generating singlet oxygen. The singlet oxygen is trapped by FFA, causing a decrease in oxygen concentration in solution, this decrease in oxygen concentration is monitored and along with the amount of light absorbed by the sensitizer can be directly applied to efficiency of the photosensitizer to accurately determine the singlet oxygen quantum yield.

The two integral pieces of equipment used in the experiment included a PTI spectrofluorometer and an Ocean Optics spectrometer outfitted with a ruthenium coated oxygen probe. The spectrofluorometer system was used as the sensitizer excitation light source and to measure the number of photons absorbed by the sensitizer per given amount of time. The oxygen probe provided the means to measure, inside the fluorometer cell within the fluorometer, the amount of oxygen converted to singlet oxygen and subsequently consumed by the singlet oxygen acceptor furfuryl alcohol.

The first step in the experiment developed to determine the singlet oxygen quantum yield involved calibrating the oxygen probe. The first attempts at calibration focused on using a vial purged and filled with pure nitrogen and subsequently capped with a rubber septum as the zero percent oxygen concentration standard. The other standard used was air, which has a known oxygen concentration of 20.8%. This procedure was later determined to be less then ideal because controlling the temperature at calibration proved to be extremely important and difficulties in the conversion of percent oxygen in air to that of mg/L or ppm in solution did not bode well with experimental data. Subsequently, further attempts were abandoned.

The problems encountered using ambient air and known gases as calibration standards were remedied by using temperature-controlled aqueous solutions bubbled with nitrogen and oxygen, respectively. Oxygen and nitrogen were each bubbled through a vial of water capped by a rubber septum for approximately two hours prior to use for calibration of the oxygen probe. The two known standards were kept at a constant temperature of 25° C with the use of a water bath. The zero mg/L standard of de-ionized water was sealed with a rubber septum. A

hypodermic needle connected to a nitrogen tank penetrated the rubber septum so that the tip of the needle was well below the water level inside the vial. A second needle was inserted into the septum but its tip was positioned so that it was well above the water level within the vial, so that it acted like a vent. The nitrogen gas was turned on so that it bubbled through the water and out the vent for approximately two hours. A solution saturated with oxygen was made by the same process, the only difference being the use oxygen in place of nitrogen.

Once the standards were made they were then used to calibrate the fiber optic oxygen probe. Two standards with differing oxygen concentrations were needed to generate a standard linear Stern-Volmer plot of emission intensity vs. oxygen concentration. The Ocean Optics user manual suggested calibrating with the lower oxygen concentrated solution first. The needle tip of the oxygen probe was inserted into the rubber-septum capped vial and left to equilibrate until the intensity reading stabilized. Equilibration typically took approximately six to eight minutes. The procedure was repeated for the vial containing the oxygen-saturated solution. The intensity readings relating to both standards were documented and recorded by the software. A linear plot of the two points was used to generate the desired calibration curve relating the emission intensity of the probe to the oxygen concentration in the surrounding environment.

Once the oxygen probe was correctly calibrated, attention was diverted to the PTI spectrofluorometer. The fluorometer was outfitted with a series of neutral density filters (NDF) to provide an adequate amount of protection to the photomultiplier tube (PMT). The spectrofluorometer was not used in its traditional sense. It was used because it had a adjustable monochromatic light source and a detector suitable for the experiment at hand. The singlet

oxygen measurements required the determination of the number of photons absorbed by the sensitizer with respect to the number of molecules of singlet oxygen generated. The emission wavelength was subsequently set so that it would be the same as the excitation wavelength. In this way, the number of photons absorbed could be determined by using of a blank reference solution void of the sensitizer to get a reference intensity reading. The number of photons absorbed could then be determined by using a second solution using the sensitizer, and subtracting the blank from the solution with the sensitizer.

Because emission intensities are typically much less intense than intensity of irradiation to excite the molecule, filters were placed in front of the PMT inlet. A triangular fluorometer cell used to house the solutions studied and the oxygen probe was purchased from Starna Cells. The orthogonal side of the triangular cell was coated with a highly reflective mirrored coating designed to redirect the light that went through the cell at 90°, through the filter, and into the PMT (Figure 8).

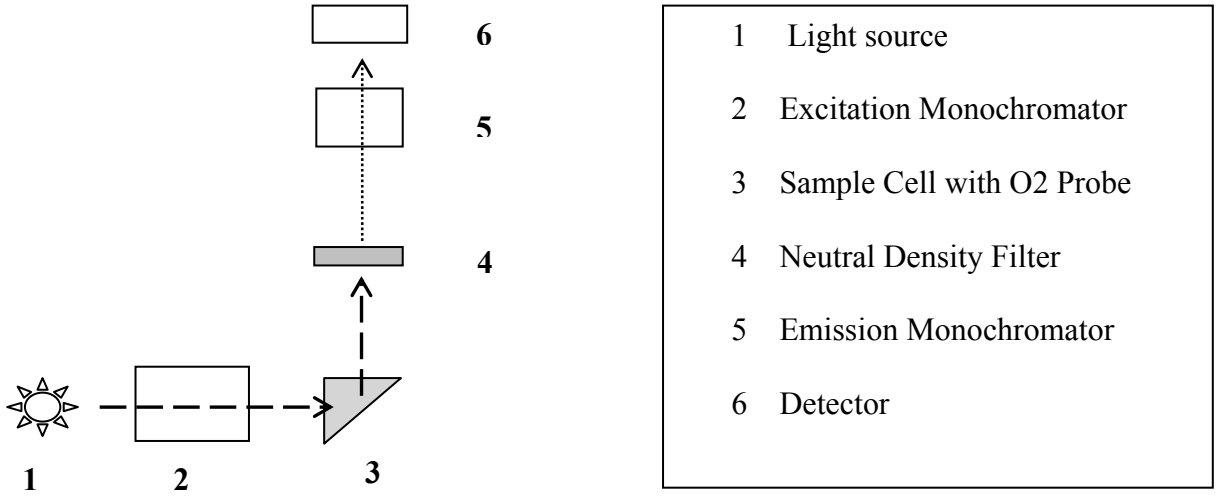

Figure 8. Diagram of experimental set-up

Solutions with the same concentration of photosensitizer and varying concentrations of FFA were made for each run. A total of eight solutions were made in all for each run (one blank with the maximum concentration of FFA and seven with decreasing concentrations of FFA). Pure oxygen was bubbled through each solution for approximately five minutes prior to use. The fluorescence cell was then filled to the top of the opening with the solution of interest. A rubber septum was placed in the opening of the cell to form an airtight seal. The oxygen probe was lowered into the fluorometer chamber via an entry port located on the lid of the fluorometer. The oxygen probe penetrated the septum so that probe was sufficiently submerged in the solution in order to measure the oxygen concentration. A magnetic stir bar kept in the fluorescence cell kept the solution adequately stirred to ensure a constant oxygen concentration throughout the entire volume of the cell. Because the solubility of oxygen in water is temperature dependent, the cell

and solution were kept at a constant temperature of 25° C with a circulating water bath to ensure consistency between subsequent runs.

Furfuryl alcohol purchased from Sigma-Aldrich was found to contain some impurities. Furfuryl alcohol was purified by distillation and the distillate was stored at 5 °C in a freezer after use. Solutions for the study were made in the following manner. All work was accomplished in the dark. Prior to each run, eight vials were cleaned, labeled, and covered with aluminum foil. A pipette was used to add 0.5-mL of the distilled FFA to 50-mL volumetric flask. The flask was then filled to capacity with de-ionized water. Approximately 0.005 grams of sensitizer, in the case of Rose Bengal, was weighed and added to a 25-mL volumetric flask and dissolved in de-ionized water. Table 2 shows the amounts of the FFA solution, sensitizer solution, and water added to each of the eight vials with the use of a volumetric pipette.

Table 2. Volume of solutions added

Solution #	FFA added (mL)	Sensitizer (mL)	Water
1	9	1	0
2	7	1	2
3	5	1	4
4	3	1	6
5	2	1	7
6	1	1	8
7	.5	1	8.5
8	9	0	1

The fiber-optic oxygen probe was then calibrated at the beginning of each day of use by the method previously described. An intensity reading from the excitation source of the fluorometer was taken and documented using a voltmeter. Oxygen was bubbled through each of the eight vials just prior to use. Solution number eight, the control without any sensitizer, was always handled first. A stir bar was added to the fluorometer cell and after exposure to approximately five minutes of pure oxygen, a portion of the solution was placed in the fluorescence cell, so that the cell was completely full. The cell was placed in the cell holder with in the reaction chamber of the fluorometer. The lid of the spectrofluorometer was lowered and a

rubber septum, already pierced by the needle tip oxygen probe, was used to as a cap for the fluorescence cell. The septum fit snuggly so that the solution was virtually airtight. The probe was placed so that it went about 1/3 of the way into the cell. The system was left in place for approximately six to seven minutes (however much time it took the oxygen probe to equilibrate and stabilize to get the initial oxygen concentration). The initial oxygen concentration was recorded and the fluorometer acquisition was initiated. The solution in the fluorescence cell was then irradiated with light for 180 seconds. The oxygen probe was once again used to determine the oxygen concentration. The oxygen concentration after irradiation was recorded and the change in oxygen concentration could then be determined by subtracting the initial concentration from the final concentration.

The approximate concentrations of two sensitizers studied and the concentrations of FFA are documented for the eight solutions used to determine the $\Delta\phi$ of each sensitizer are shown in Table 3.

Table 3. Concentrations of solutions in experiment

Solution #	FFA (mM)	Rose Bengal (μM)	Compound 3 (μM)
1	104	980	156
2	89.0	980	156
3	57.9	980	156
4	34.7	980	156
5	23.1	980	156
6	11.6	980	156
7	5.8	980	156
8	104	0	0

RESULTS AND DISCUSSION

Although compound **3** possesses an absorption maximum in the UV region of the electromagnetic spectrum it was studied, not for use with respect to single photon excitation, but because of its potential for use in two-photon PDT. The UV/Vis spectrum shown in Figure 9 reveals that compound **3** has a λ_{max}, near 363 nm. This could allow for an excitation wavelength near 730 nm, well within the 700-900 nm region that is necessary to ensure greater light penetration into the tissue.

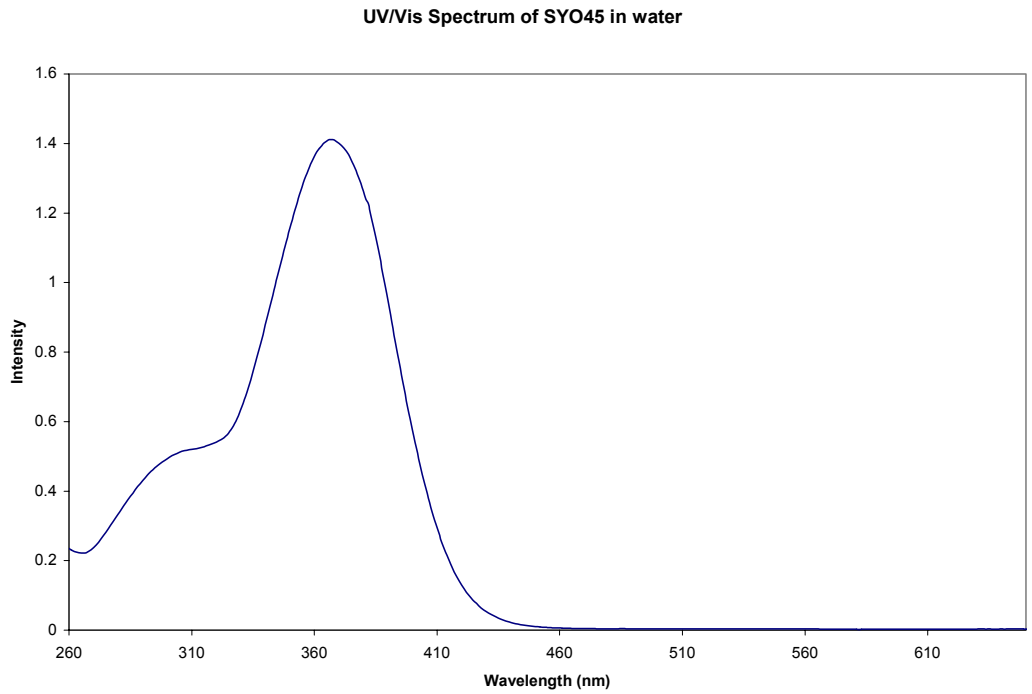

Figure 9. UV/Vis spectrum of compound **3**

During the course of validating the experiment, it was found that the reagent grade FFA purchased from Sigma-Aldrich contained a significant amount of impurities. This was apparent when considering that FFA has an absorption maximum around 215 nm and the FFA solution had a notable yellow tint to it. The UV/VIS spectrum of the stock solution showed the presence of two absorption maximum, one at 215 nm and a second at 270 nm (Figure 10). The stock solution of FFA purchased from Sigma-Aldrich was purified by distillation. Even at very dilute concentrations, ~200μM, the spectra in Figure 10 show the presence of the second peak at 270 nm and the subsequent disappearance of the impurity after distillation.

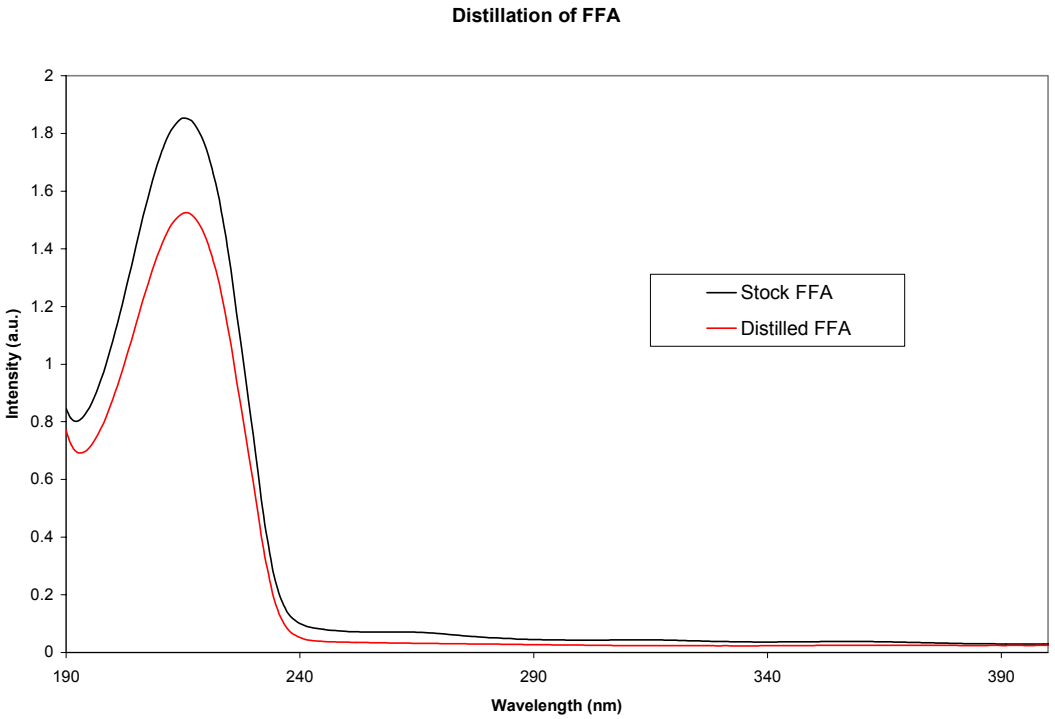

Figure 10. UV/Vis absorbance of Stock FFA and FFA purified by distillation

The technique used to determine the singlet oxygen quantum yields of different

sensitizers was first validated with the use of a standard sensitizer, Rose Bengal, which has a known and well documented singlet oxygen quantum yield value. Its singlet oxygen quantum yield has been reported to range from between 0.7 to 0.8 in aqueous media.[33] In order to determine the appropriate wavelength needed to irradiate the sensitizer, the UV/Vis spectrum of the Rose Bengal was taken and the spectrum is shown in Figure 11 below. Rose Bengal (RB) was found to possess an absorption maximum, λ_{max}, at approximately 549 nm.

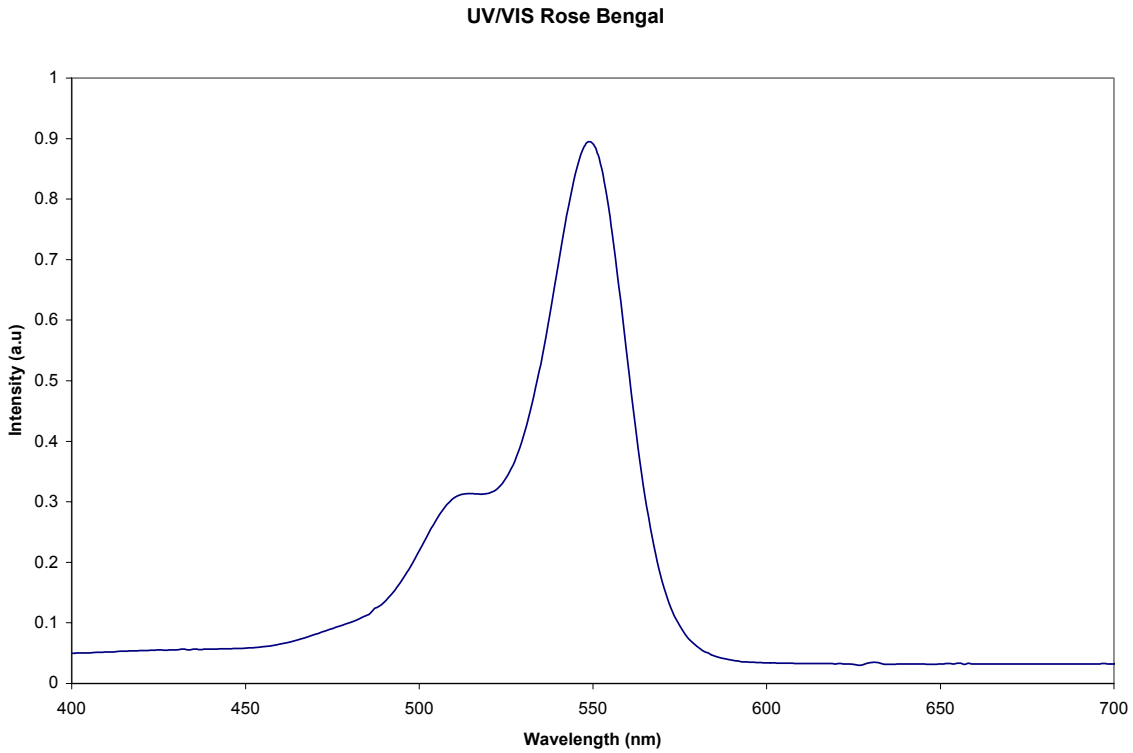

Figure 11. UV/Vis spectrum of Rose Bengal

As discussed in the experimental section, the number of photons absorbed by the sensitizer was determined by using a spectrofluorometer. The eight different solutions necessary

for each run were made and the solutions were then irradiated at the λ_{max} of the sensitizer, the wavelength in which the most light would be absorbed by the sensitizer and subsequently the solution. The following graph (Figure 12) was used to determine the number of photons absorbed by the sensitizer in each solution upon irradiation at 549 nm. Eight runs, corresponding to the eight solutions were made as previously described with varying concentrations of FFA and a constant concentration of RB, were evaluated and are plotted on the graph below. Figure 12 shows the data detected by the PMT, plotted as counts/sec over a time period of 180 seconds.

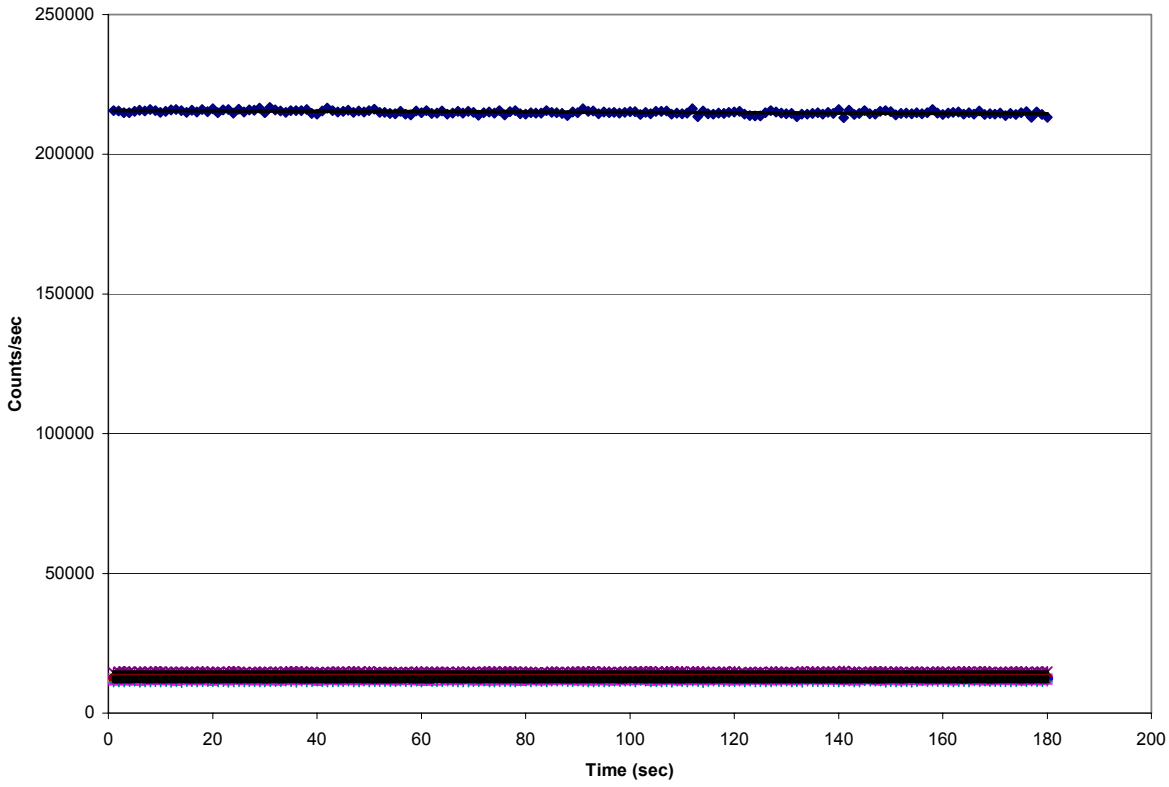

Figure 12. Data acquired from run #1 in PMT with RB as sensitizer

The reference blank, the solution without the sensitizer RB, accounts for a single run

giving a substantially higher counts/sec compared to the other seven runs overlapping and possessing much lower counts/sec marks. The number of photons absorbed by the sensitizer was calculated by subtracting the intensity (count/sec) of each solution from that of the blank, converting count/sec to photons/sec (based on the wavelength of light used), and multiplying by the number of seconds the sensitizer was exposed to the light. An example of the calculations for this experiment are shown in the Appendix.

The initial and final oxygen concentrations for each solution were determined both before and after irradiation. The oxygen concentration values for run #1 are shown in Table 4.

Table 4. Oxygen consumption data for run #1 with RB

Solution #	$[O_2]$ initial (mg/L)	$[O_2]$ final (mg/L)	$\Delta [O_2]$
1	40.37	34.45	5.92
2	39.97	35.77	4.20
3	40.72	37.37	3.35
4	40.97	38.04	2.93
5	40.66	38.37	2.29
6	38.01	36.98	1.03
7	30.88	30.37	0.51
8	40.9	40.8	0.1

The change in oxygen concentration was then converted to the number of molecules of

oxygen consumed. This calculation was accomplished based on the known volume of the triangular cell.

Equations 17 and 18 were previously explained. They demonstrated the relationship of the quantum yield of photooxidation of the singlet oxygen acceptor to that of the singlet oxygen quantum yield of the sensitizer. When the singlet oxygen acceptor concentration, [FFA], is much larger than the concentration of the sensitizer then the quantum yield of photooxidation was shown to be dependent upon the number of photons absorbed by the sensitizer and the corresponding number of molecules of oxygen that reacted to form AO_2. The singlet oxygen quantum yield could be calculated once these parameters were determined experimentally. The y-intercept of the plot of the inverse of the concentration of the singlet oxygen acceptor at various concentrations vs. the inverse of the experimentally determined quantum yield of photooxidation is proportional to the singlet oxygen quantum yield of the photosensitizer involved in the study. The experimentally derived values for run #1 are shown below in Table 5.

Table 5. Data for $\Delta\phi$ plot

1/[A]	# photons/molecules O_2
9.606147935	3.54E+00
12.34567901	5.01E+00
17.2860847	6.24E+00
28.81014117	7.06E+00
43.21521175	9.12E+00
86.43042351	2.03E+01
172.860847	4.11E+01

The plot of the data shown in Table 5 is shown in Figure 13. The y-intercept of the plot was experimentally determined to be equal to 1.1508. From the set of equations previously described relating the photooxidation of the acceptor to that of the $\Delta\phi$ of the sensitizer, the y-intercept from the plot is known to be proportional to the singlet oxygen quantum yield through the relationship $1/[\Delta\phi(\alpha)]$. The term α is an experimentally derived coefficient for FFA in specific solutions. It was reported to be 1.23 ± 0.02 for FFA in water.[46] Knowing this value, run #1 was determined to give a $\Delta\phi$ value of 0.71 for the photosensitizer Rose Bengal.

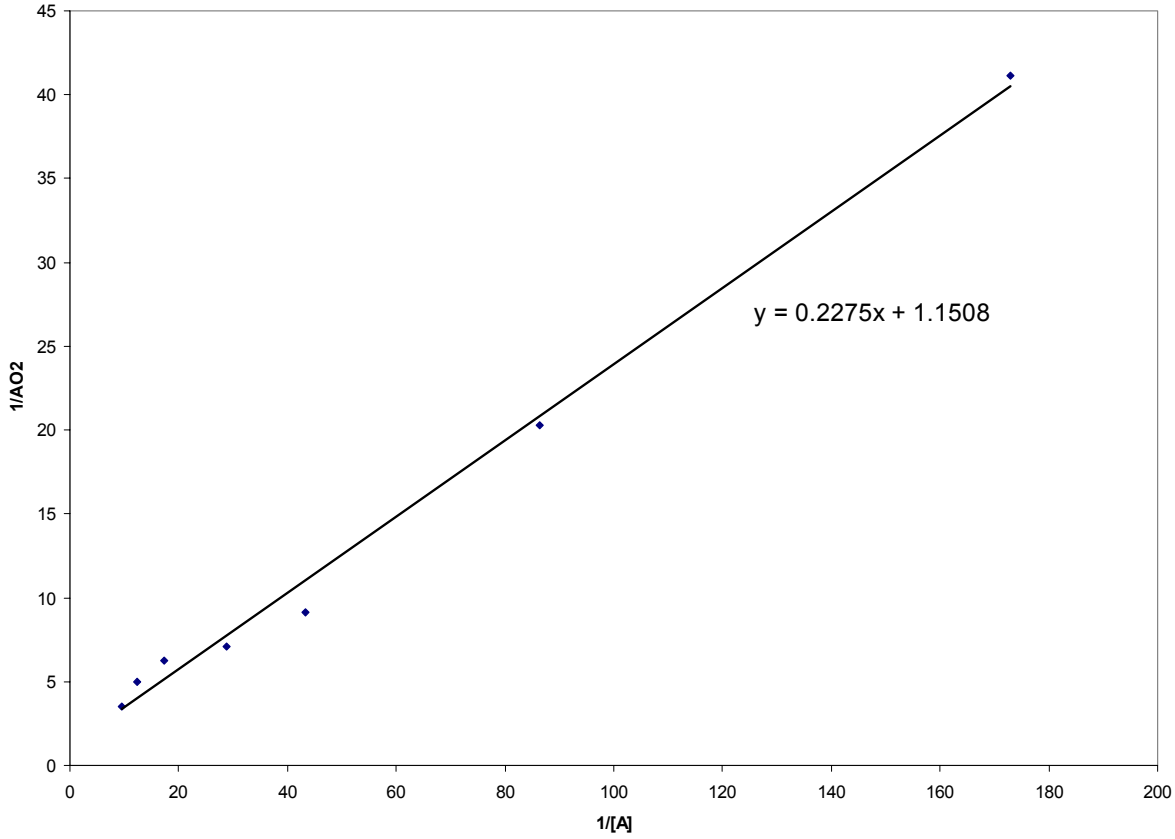

Figure 13. Determination of $\Delta\phi$ for RB

The data resulting from a total of three successful runs using RB as the sensitizer are documented with Table 6. The average $\Delta\phi$ value for the three runs was determined to be 0.71. This value is within agreement with accepted literature values for Rose Bengal in water found to range from 0.7 to 0.8. The standard deviation was calculated to be ±0.05. Each of the values from the three runs were within one standard deviation of the average singlet oxygen quantum yield. This fact gives greater credence to the repeatability of the experiment.

Table 6. $\Delta\phi$ Results for RB

Run #	1	2	3
$\Delta\phi$	0.71	0.76	0.67

The agreement between literature and experimental values for Rose Bengal validate the overall experiment. Subsequently experiments were run for the new photosensitizer, synthesized by Dr. Belfield's research group using the same procedures. The data for the three runs is located in the Appendix. The average singlet oxygen quantum yield was calculated to be 0.18. The standard deviation was determined to be ±0.03 (Table 7).

Table 7. $\Delta\phi$ Results for SYO45

Run #	1	2	3
$\Delta\phi$	0.16	0.16	0.21

Once again the values from the three runs fall within one standard deviation of the average singlet oxygen quantum yield of 0.18, providing confidence in the accuracy of the data and technique.

CONCLUSIONS AND FUTURE WORK

A new method for the determination of singlet oxygen quantum yields for water-soluble photosensitizers in aqueous environments was demonstrated and validated. The method was shown to be reproducible and in agreement with literature. Additionally the $\Delta\phi$ of a new water-soluble sensitizer was evaluated and measured.

This demonstrated capability now provides a relatively fast method to measure the singlet oxygen quantum yields of other water-soluble sensitizers. The new sensitizer studied in water was a modified version (hydrophilic analogue) of a sensitizer that was studied previously. The carboxylic acid functional groups were added to the compound in order to increase its solubility in water. Further modifications can be made to the organic sensitizers synthesized by the research group in an attempt to identify a photosensitizer that performs well in aqueous media.

The ultimate goal, once a candidate sensitizer with a high is discovered, will be to perform *in vivo* studies involving real cells and tissue.

APPENDIX: EXAMPLE CALCULATIONS AND DATA

The following is a set of example equations for Run #1 using the sensitizer Rose Bengal. A power meter was used to measure the intensity of the light coming from the excitation light source. In this case the intensity was measured to be 420 $\mu W/cm^2$. The energy of a photon is related to the wavelength by Planck's equation:

$$E = hc/\lambda \qquad (20)$$

where: $h = 6.626 \times 10^{-34}$ J/s and $c = 3.0 \times 10^{8}$ m/s. The number of photons from the excitation source can then be calculated by:

$E = 0.00042$ W W/cm^2		
÷ by 6.626×10^{-34} J/s	=	6.34×10^{29} $W/J \cdot s \cdot cm^2$
÷ by 3.0×10^{8} m/s (seconds cancel out)	=	2.11×10^{21} $W/J \cdot m \cdot cm^2$
x by 549×10^{-9} m (meters cancel out)	=	1.16×10^{15} $W/J \cdot cm^2$
x by ($10{,}000$ $cm^2/1$ m^2)	=	1.16×10^{19} $W/J \cdot m^2$
x by the area (0.00042 m^2)	=	4.87×10^{15} W/J
1 Watt = 1 J/s ∴	=	4.87×10^{15} photons/s

The number of photons/s absorbed by the sensitizer is then calculated from the plot generated from the PMT. The y-intercept from the plot of the counts/sec vs. time give the average number of counts registered by the PMT. A ratio is set up so that:

$$I_{Pb} / C_b = I_{Ps} / C_s \qquad (21)$$

where I_{Pb} is the intensity of photons/s for the reference (the number just calculated) and C_b is the number of number of counts/s recorded by the PMT for that same solution, I_{Ps} is the number of photons/s for the unknown solution, and C_s are the counts/s recorded by the PMT for that same unknown solution. The calculation is as follows:

$$(4.87 \times 10^{15} \text{ photons/sec}) / 215588 \text{ counts/sec} = (\text{x photons/sec}) / 12321 \text{ counts/sec}$$

Solving for x gives 2.78×10^{14} photons/sec. This step is repeated for the other six solutions and the number of photons absorbed are then calculated by subtracting the intensity (number) of photons for each solution from that of the blank solution and multiplying by the number of seconds of irradiation. The number of photons/sec absorbed are then calculated by:

$$(4.87 \times 10^{15} \text{ photons/sec} - 2.78 \times 10^{14} \text{ photons/sec}) \times 180 \text{ sec} = 8.27 \times 10^{17} \text{ photons}$$

Table 8 shows the calculations for the entire run.

Table 8. Determination of the number of photons absorbed for run #1 with RB

Solution #	[FFA]	count/s	Photons/s	p-absorbed/s	Seconds	p-absorbed
1	0.1041	12321	2.78E+14	4.59E+15	180	8.27E+17
2	0.081	11232	2.54E+14	4.62E+15	180	8.31E+17
3	0.05785	12455	2.81E+14	4.59E+15	180	8.26E+17
4	0.03471	14724	3.33E+14	4.54E+15	180	8.17E+17
5	0.02314	12649	2.86E+14	4.59E+15	180	8.25E+17
6	0.01157	12765	2.88E+14	4.58E+15	180	8.25E+17
7	0.005785	11882	2.69E+14	4.60E+15	180	8.29E+17

The second part of the experiment involved calculating the number of molecules of oxygen consumed. This was accomplished subtracting the final concentration from the initial concentration. This was then multiplied by the volume of the sample and divided by the molar mass of oxygen to get the number of moles. The number of moles were then converted to molecules by using Avagadro's constant.

(40.37 mg/L) – (34.45 mg/L) = 5.92 mg/L

x by 0.0021 L (volume of cuvette) = 0.01243 mg

÷ by 1000 to convert to grams = 1.243×10^{-5} g

÷ by 31.998 g/mol = 3.89×10^{-7} mol

x by 6.02×10^{23} molecules/mol = 2.34×10^{17} molecules

Table 9 shows the results for the calculation of the number of molecules of oxygen consumed for all seven solutions in run #1.

Table 9. Determination of the # of molecules of O_2 consumed for run #1 with RB

Solution #	O_2 initial (mg/L)	O_2 final (mg/L)	Delta (mg/L)	O_2 consumed (mg)	moles O_2	Molecules
1	40.37	34.45	5.92	0.012432	3.89E-07	2.34E+17
2	39.97	35.77	4.2	0.00882	2.76E-07	1.66E+17
3	40.72	37.37	3.35	0.007035	2.20E-07	1.32E+17
4	40.97	38.04	2.93	0.006153	1.92E-07	1.16E+17
5	40.66	38.37	2.29	0.004809	1.50E-07	9.05E+16
6	38.01	36.98	1.03	0.002163	6.76E-08	4.07E+16
7	30.88	30.37	0.51	0.001071	3.35E-08	2.01E+16

Once all the calculations were made, a plot of 1/[A] vs. (# of photons absorbed/molecules of oxygen consumed) gave the graph illustrated in Figure 13, in Results and Discussion section.

Rose Bengal Run #2:

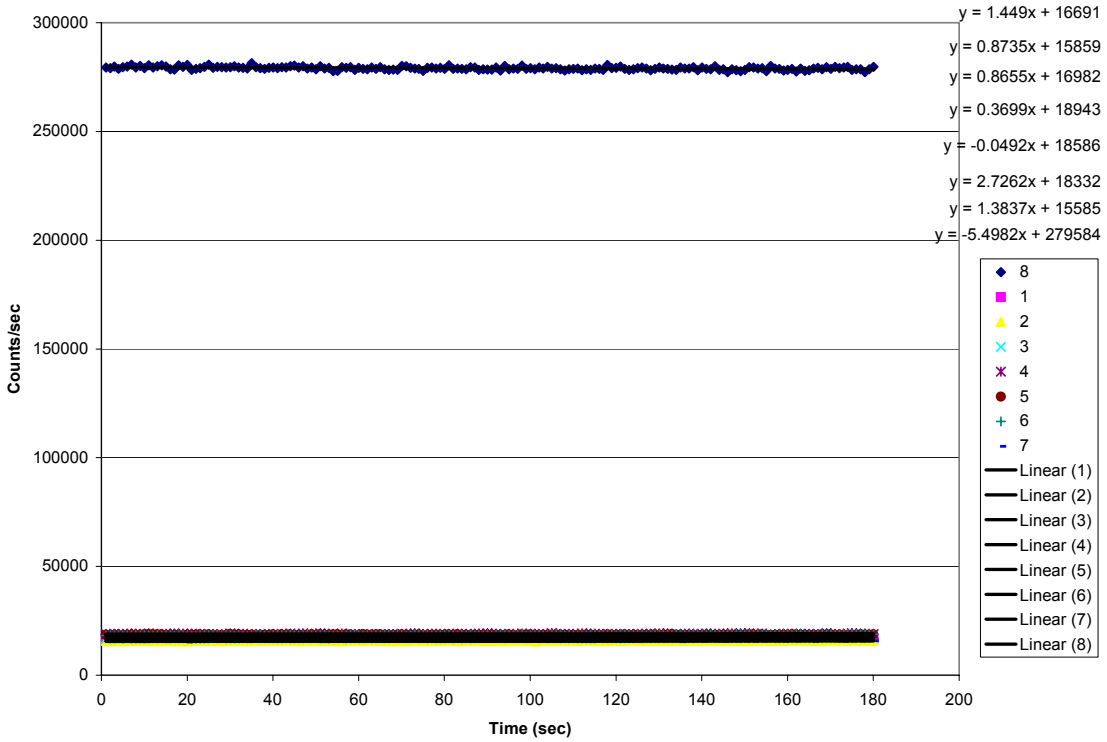

Figure 14. Plot to determine the number of photons absorbed for run #2 with RB

Table 10. Determination of the number of photons absorbed for run #2 with RB

Solution #	[FFA]	Count/s	Photons/s	p-absorbed/s	secs	p-absorbed
1	0.1041	16691	3.12E+14	4.91E+15	180	8.83E+17
2	0.081	15859	2.96E+14	4.92E+15	180	8.86E+17
3	0.05785	16982	3.17E+14	4.90E+15	180	8.83E+17
4	0.03471	18943	3.54E+14	4.87E+15	180	8.76E+17
5	0.02314	18586	3.47E+14	4.87E+15	180	8.77E+17
6	0.01157	18332	3.42E+14	4.88E+15	180	8.78E+17
7	0.005785	15585	2.91E+14	4.93E+15	180	8.87E+17

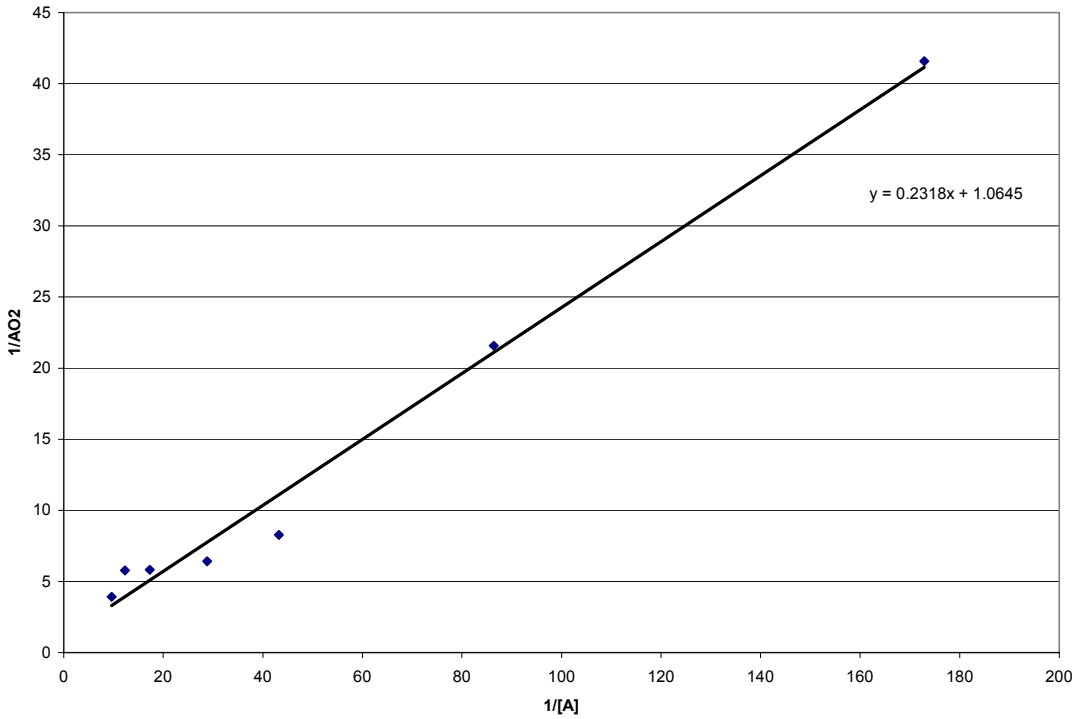

Figure 15. Determination of $\Delta\phi$ for RB

Table 11. Determination of the # of molecules of O_2 consumed for run #2 with RB

Solution #	O_2 initial (mg/L)	O_2 final (mg/L)	Delta (mg/L)	O_2 consumed (mg)	Moles O_2	Molecules
1	37.15	31.43	5.72	0.012012	3.75E-07	2.26E+17
2	35.54	31.65	3.89	0.008169	2.55E-07	1.54E+17
3	36.34	32.5	3.84	0.008064	2.52E-07	1.52E+17
4	39.6	36.15	3.45	0.007245	2.26E-07	1.36E+17
5	40.03	37.35	2.68	0.005628	1.76E-07	1.06E+17
6	41.3	40.27	1.03	0.002163	6.76E-08	4.07E+16
7	38.48	37.94	0.54	0.001134	3.54E-08	2.13E+16

Rose Bengal Run # 3:

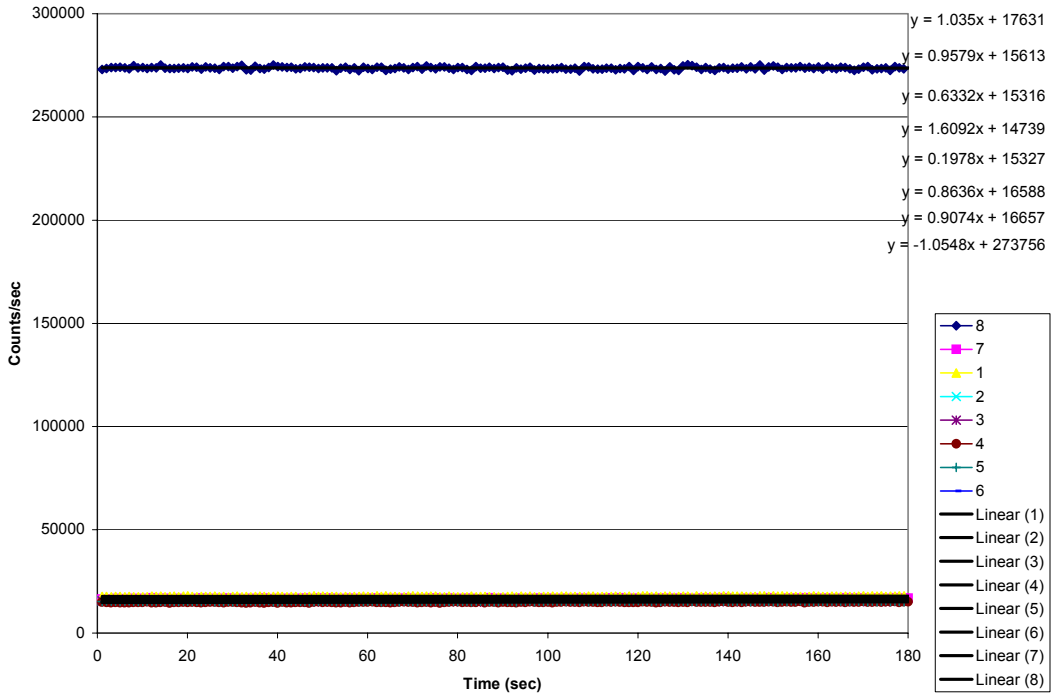

Figure 16. Plot to determine the number of photons absorbed for run #3 with RB

Table 12. Determination of the number of photons absorbed for run #3 with RB

Solution #	[FFA]	count/s	Photons/s	p-absorbed/s	secs	p-absorbed
1	0.1041	17631	3.21E+14	4.67E+15	180	8.40E+17
2	0.081	15613	2.84E+14	4.70E+15	180	8.47E+17
3	0.05785	15316	2.79E+14	4.71E+15	180	8.48E+17
4	0.03471	14739	2.69E+14	4.72E+15	180	8.49E+17
5	0.02314	15327	2.79E+14	4.71E+15	180	8.48E+17
6	0.01157	16588	3.02E+14	4.69E+15	180	8.43E+17
7	0.005785	16657	3.03E+14	4.68E+15	180	8.43E+17

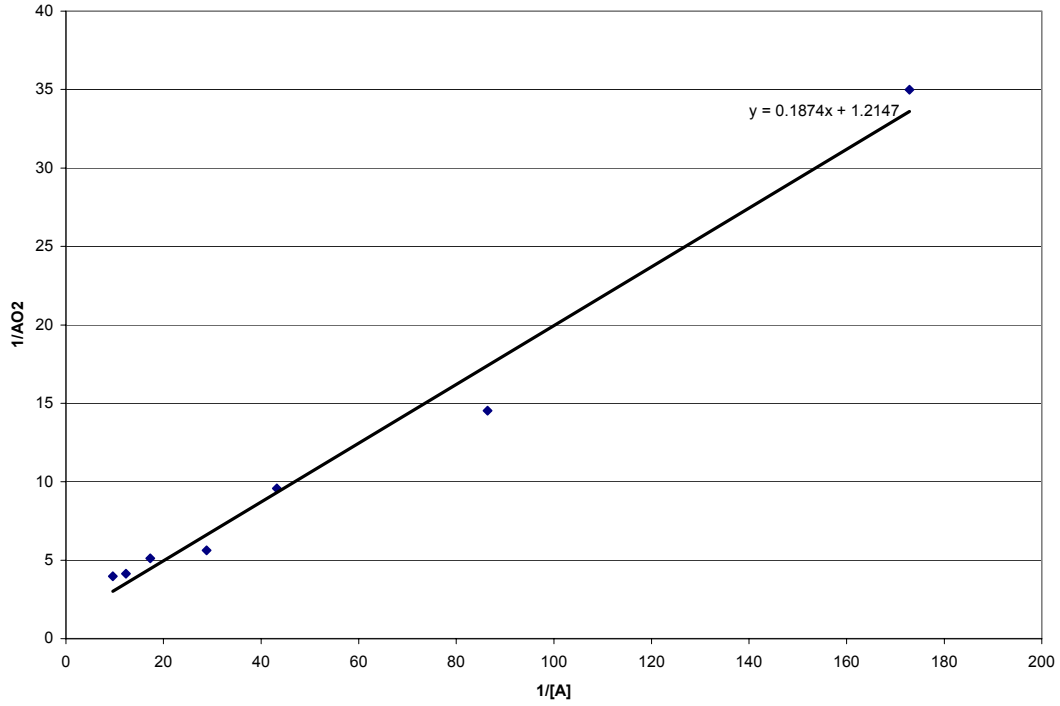

Figure 17. Determination of $\Delta\phi$ for RB

Table 13. Determination of the # of molecules of O_2 consumed for run #3 with RB

Solution #	O_2 initial (mg/L)	O_2 final (mg/L)	Delta (mg/L)	O_2 consumed (mg)	moles O_2	Molecules
1	40.08	34.74	5.34	0.011214	3.50E-07	2.11E+17
2	37.37	32.19	5.18	0.010878	3.40E-07	2.05E+17
3	39.39	35.19	4.2	0.00882	2.76E-07	1.66E+17
4	37.52	33.7	3.82	0.008022	2.51E-07	1.51E+17
5	36.31	34.07	2.24	0.004704	1.47E-07	8.85E+16
6	38.01	36.54	1.47	0.003087	9.65E-08	5.81E+16
7	36.97	36.36	0.61	0.001281	4.00E-08	2.41E+16

SYO45 Run #1

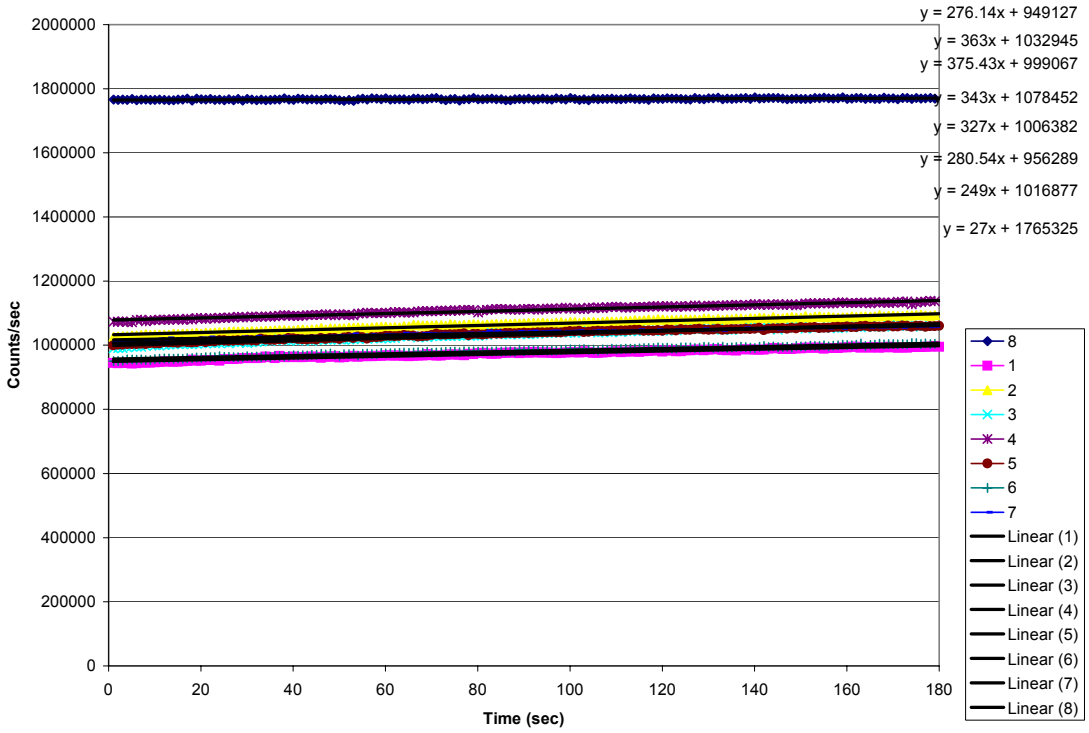

Figure 18. Plot to determine # of photons absorbed for run #1 for SYO45

Table 14. Determination of the number of photons absorbed for run #1 for SYO45

Solution #	[FFA]	count/s	photons/s	p-absorbed/s	secs	p-absorbed
1	0.1041	949127	1.32E+15	1.13E+15	180	2.04E+17
2	0.081	1032945	1.44E+15	1.02E+15	180	1.83E+17
3	0.05785	999067	1.39E+15	1.07E+15	180	1.92E+17
4	0.03471	1078452	1.50E+15	9.55E+14	180	1.72E+17
5	0.02314	1006382	1.40E+15	1.06E+15	180	1.90E+17
6	0.01157	956289	1.33E+15	1.12E+15	180	2.02E+17
7	0.00579	1016877	1.41E+15	1.04E+15	180	1.87E+17

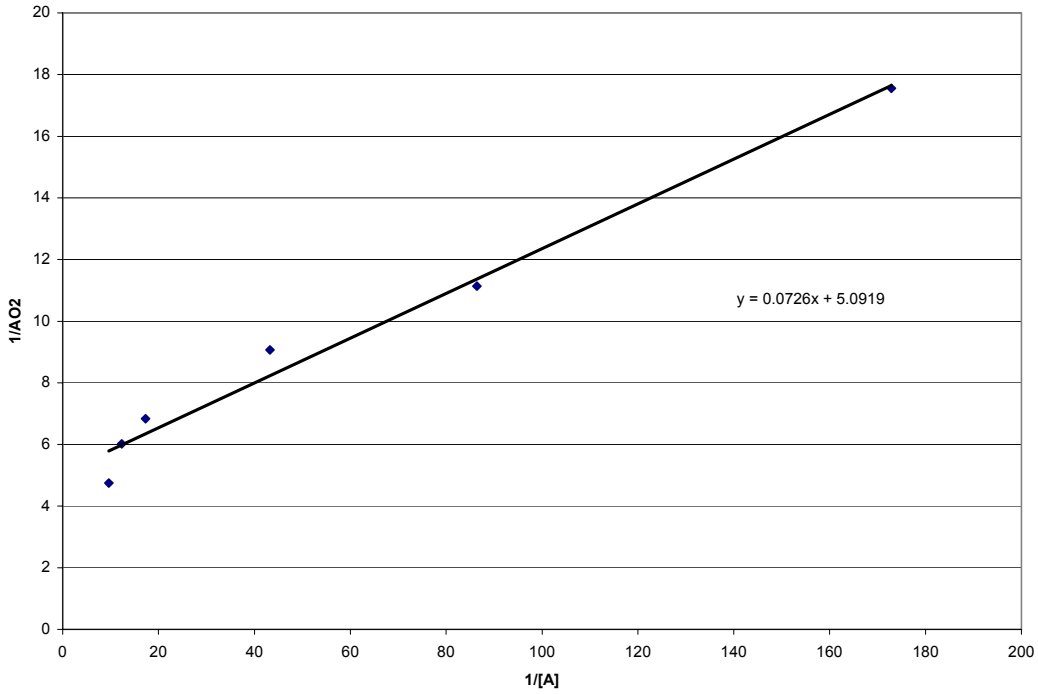

Figure 19. Determination of $\Delta\phi$ for SYO45

Table 15. Data of the number of molecules of O_2 consumed for run #1 with SYO45

Solution #	O_2 initial (mg/L)	O_2 final (mg/L)	Delta (mg/L)	O_2 consumed (mg)	Moles O_2	Molecules
1	38.88	37.79	1.09	0.002289	7.15E-08	4.31E+16
2	38.6	37.83	0.77	0.001617	5.05E-08	3.04E+16
3	34.88	34.17	0.71	0.001491	4.66E-08	2.81E+16
4	38.26	37.4	0.86	0.001806	5.64E-08	3.40E+16
5	37.33	36.8	0.53	0.001113	3.48E-08	2.09E+16
6	35.4	34.94	0.46	0.000966	3.02E-08	1.82E+16
7	33.7	33.43	0.27	0.000567	1.77E-08	1.07E+16
8	40	39.8	0.2	0.00042	1.31E-08	7.90E+15

Run # 2 SYO45

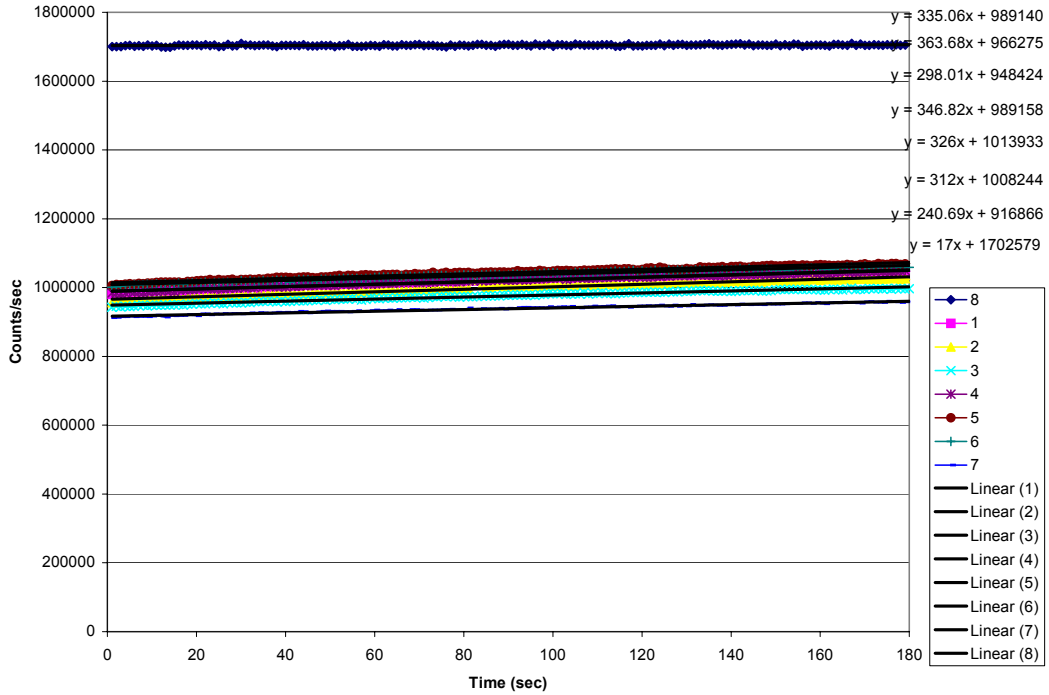

Figure 20. Plot to determine # of photons absorbed for run #2 for SYO45

Table 16. Determination of the number of photons absorbed for run #2 for SYO45

Solution #	[FFA]	count/s	Photons/s	p-absorbed/s	Secs	p-absorbed
1	0.1041	989140	1.34E+15	9.64E+14	180	1.74E+17
2	0.081	966275	1.31E+15	9.95E+14	180	1.79E+17
3	0.05785	948424	1.28E+15	1.02E+15	180	1.83E+17
4	0.03471	989158	1.34E+15	9.64E+14	180	1.74E+17
5	0.02314	1013933	1.37E+15	9.31E+14	180	1.68E+17
6	0.01157	1008244	1.36E+15	9.38E+14	180	1.69E+17
7	0.005785	916866	1.24E+15	1.06E+15	180	1.91E+17

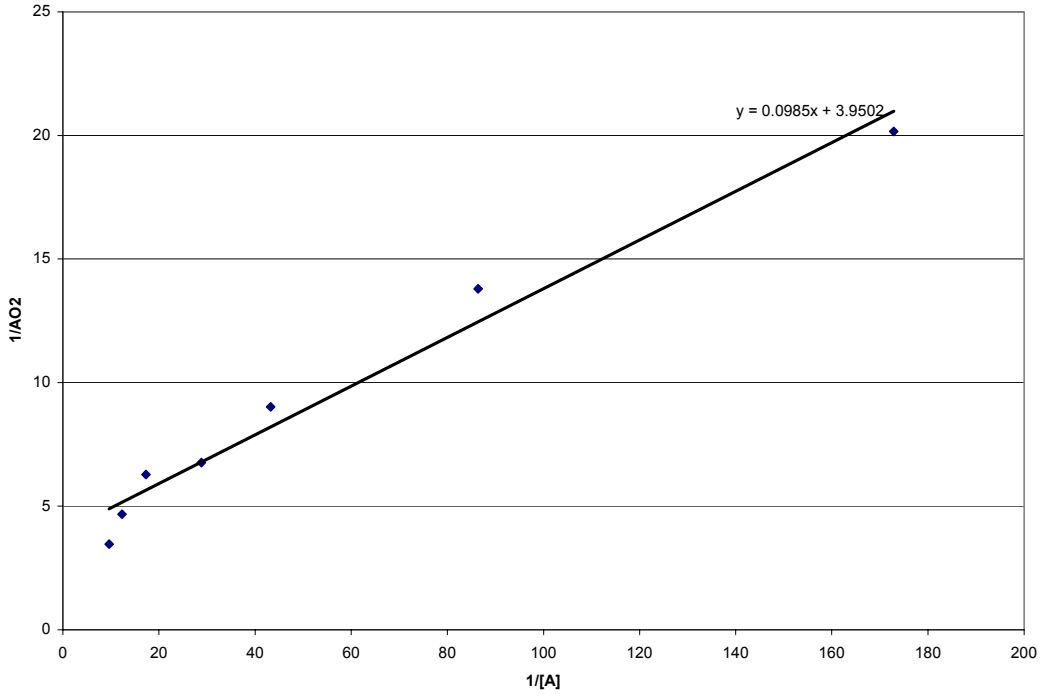

Figure 21. Determination of $\Delta\phi$ for SYO45

Table 17. Data of the number of molecules of O_2 consumed for run #2 with SYO45

Solution #	O_2 initial (mg/L)	O_2 final (mg/L)	Delta (mg/L)	O_2 consumed (mg)	Moles O_2	Molecules
1	34.4	33.13	1.27	0.002667	8.33E-08	5.02E+16
2	32.1	31.13	0.97	0.002037	6.37E-08	3.83E+16
3	35.07	34.33	0.74	0.001554	4.86E-08	2.92E+16
4	26.4	25.75	0.65	0.001365	4.27E-08	2.57E+16
5	35.04	34.57	0.47	0.000987	3.08E-08	1.86E+16
6	32.11	31.8	0.31	0.000651	2.03E-08	1.22E+16
7	31.65	31.41	0.24	0.000504	1.58E-08	9.48E+15
8	35.21	35.05	0.16	0.000336	1.05E-08	6.32E+15

Run #3 SYO45

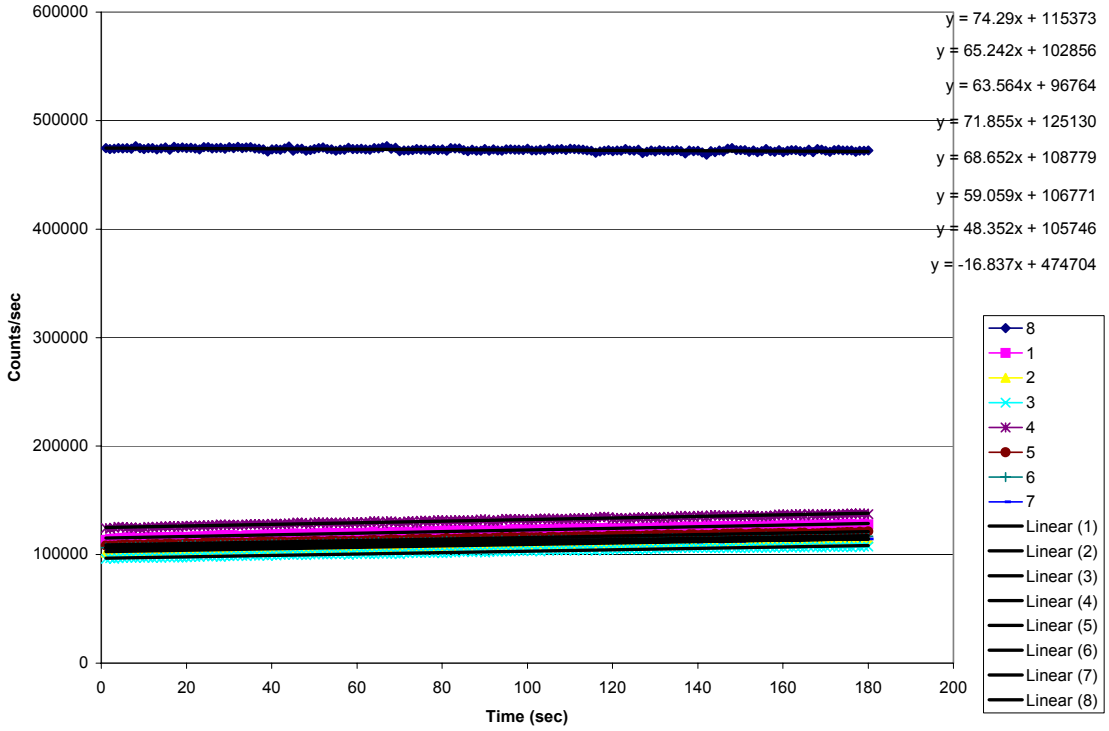

Figure 22. Plot to determine the # of photons absorbed for run #3 for SYO45

Table 18. Determination of the number of photons absorbed for run #3 for SYO45

Solution #	[FFA]	count/s	photons/s	p-absorbed/s	Secs	p-absorbed
1	0.1041	115373	5.78E+14	1.80E+15	180	3.24E+17
2	0.081	102856	5.15E+14	1.86E+15	180	3.35E+17
3	0.05785	96764	4.85E+14	1.89E+15	180	3.41E+17
4	0.03471	125130	6.27E+14	1.75E+15	180	3.15E+17
5	0.02314	108779	5.45E+14	1.83E+15	180	3.30E+17
6	0.01157	106771	5.35E+14	1.84E+15	180	3.32E+17
7	0.005785	105746	5.30E+14	1.85E+15	180	3.33E+17

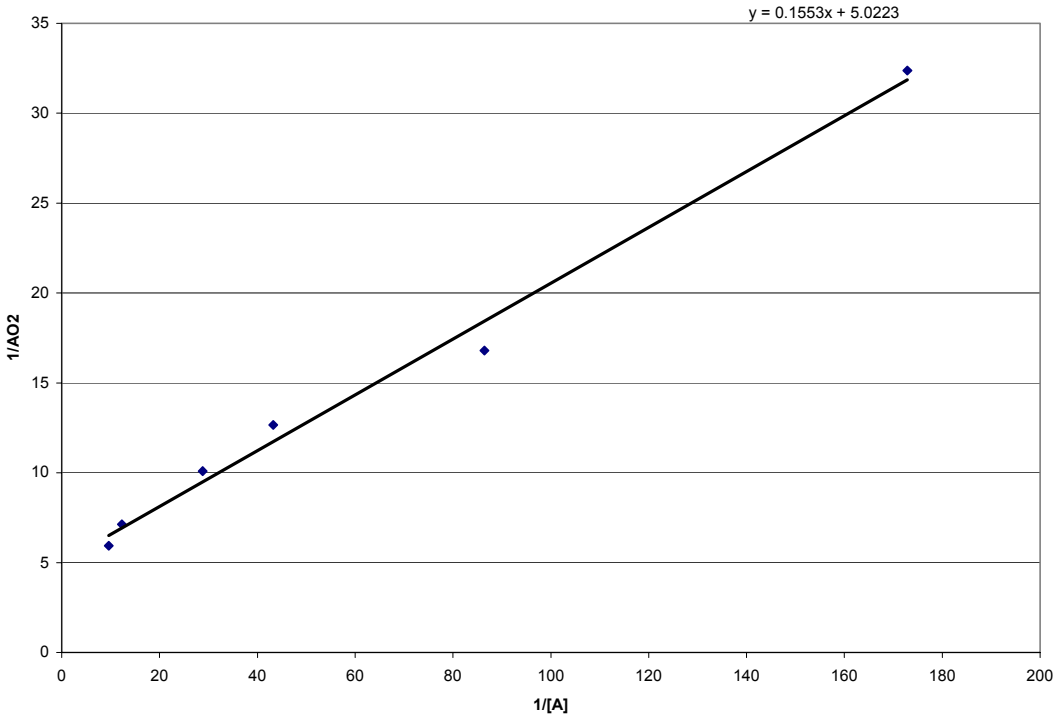

Figure 23. Determination of $\Delta\phi$ for SYO45

Table 19. Data of the number of molecules of O_2 consumed for run #3 with SYO45

Solution #	O_2 initial (mg/L)	O_2 final (mg/L)	Delta (mg/L)	O_2 consumed (mg)	Moles O_2	Molecules
1	35.4	34.02	1.38	0.002898	9.06E-08	5.45E+16
2	37.4	36.21	1.19	0.002499	7.81E-08	4.70E+16
3	34.96	34.2	0.76	0.001596	4.99E-08	3.00E+16
4	35.56	34.77	0.79	0.001659	5.18E-08	3.12E+16
5	37.5	36.84	0.66	0.001386	4.33E-08	2.61E+16
6	36.51	36.01	0.5	0.00105	3.28E-08	1.98E+16
7	37.33	37.07	0.26	0.000546	1.71E-08	1.03E+16

LIST OF REFERENCES

1. Ceburkov, O.; Gollnick, H. *European Journal of Dermatology* **2000,** *10(7)*, 568-76.

2. Konan Y. N.; Gurny, R.; Alleman, E. State of the art in the delivery of photosensitizers for photodynamic therapy. *J. Photochem. Photobiol. B: Biology* **2002**, *66*, 89-106.

3. MacDonald, I.; Dougherty, T. Basic principles of photodynamic therapy. *J. Porphyrins Phthalocyanines.* **2001**, *5(2)*, 105-129.

4. Jori, G. Tumour photosensitizers: approaches to enhance the selectivity and efficiency of photodynamic therapy. *J. Photochem. Photobiol. B: Biology* **1996**, *36*, 87-93.

5. Bonnett. R. *Chemical Aspects of Photodynamic Therapy*; Gordon and Breach Science Publishers: Netherlands, 2000; Vol 1.

6. Ochsner, M. Photophysical and photobiological processes in the photodynamic therapy of tumors. *J. Photochem. Photobiol. B: Biology*, **1997**, *39*, 1-18.

7. Stilts, Corey E.; Nelen, M.I.; Hilmey, D.G.; Davies, S.R. Water-soluble, core-modified porphyrins as novel, longer-wavelength-absorbing sensitizers for photodynamic therapy. *J. Med. Chem.* **2000**, *43*, 2403-2410.

8. Leonard, Kristi A.; Nelen, M.I.; Anderson, L. Detty, M.R. 2,4,6-Triarylchalcogenopyrylium dyes related in structure to the antitumor agent AA1 as vitro sensitizers for the photodynamic therapy of cancer. *J. Med. Chem.* **1999**, *42*, 3942-3952.

9. You, Y.; Gibson, S.; Hilf, R.; Davies S., Detty M.R. Water soluble, core-modified porphyrins. 3. Synthesis, photophysical properties, and in vitro studies of photosensitization, uptake, and localization with carboxylic acid-substituted derivatives. *J. Med. Chem.* **2003**, *46(17)*, 3734-3747.

10. Hilmey, D. G.; Masako, A.; Nelen M.I.; Stilts, C.; Detty, M.R. Water soluble, core-modified porphyrins as novel, longer-wavelength-absorbing sensitizers for photodynamic therapy II. Effects of core heteroatoms and *meso*-substituents on biological activity. *J. Med. Chem.* **2002**, *45*, 449-461.

11. Brown, J. E.; Brown, S. B.; Vernon, D. I. Cancer treatment and photodynamic therapy: opportunities and limitations. *Advances in Colour Science and Technology*. **2001**, *4(4)*, 108-116.

12. Briviba, K; Klotz L.O; Sies, H. Toxic and signaling effects of photochemically or chemically generated singlet oxygen in biological systems. *Bio. Chem.* **1997**, *378*, 1259-1265.

13. Freeriksen, P. K. Two-photon photosensitized production of singlet oxygen. *J. Am. Chem. Soc.* **2001**, *123*, 1215-1221.

14. Belfield, K. D. Two-photon organic photochemistry. *The Spectrum* **2001**, *14*, 1-7.

15. Hasan, T.; Moor, A.; Ortel, B. Photodynamic therapy of cancer. *Principles of Radiation Oncology* **2000**, 489-502.

16. Tanielian, C.; Schweitzer, C.; Mechin, R.; Wolff, C. Quantum yield of singlet oxygen production by monomeric and aggregated forms of hematoporphyrin derivative. *Free Radical Biology and Medicine* **2001**, *30*, 208-212.

17. Rotiman, L.; Ehrenberg, B.; Kobayashi, N. Spectral properties and absolute determination of singlet oxygen production yield by naphthaloporphyrins *J. Photochem. Photobiol. A: Chem.*, **1994**, *77*, 23-28.

18. Zane, C. *Photodynamic Therapy and Fluorescence Diagnosis in Dermatology*; Calzavera-Pinton, P. G.; Szeimies. R. M.; Ortel, B., Eds.; Elsevier Science: Amsterdam, The Netherlands,

2001, 101-112.

19. Redmond, R. W. Enhancement of the sensitivity of radiative and non-radiative detection techniques in the study of photosensitization by water-soluble sensitizers using a reversible micelle system. *Photochem. Photobiol.* **1991**, *54*, 547-556.

20. Bracleleon, L; Moseley, H. Laser and Non-laser Light Sources for Photodynamic Therapy *Lasers Med. Sci.* **2002**, *17*, 173-186.

21. Baumler, W. *Photodynamic Therapy and Fluorescence Diagnosis in Dermatology*; Calzavera-Pinton, P. G.; Szeimies. R. M.; Ortel, B., Eds.; Elsevier Science: Amsterdam, The Netherlands, 2001, 83-98.

22. Belfield, K. D.; Hagan, D.J.; Van Stryland, E.; Schafer, K.; Negres, R.A. New two-photon absorbing fluorene derivatives: synthesis and nonlinear optical characterization. *Organic Letters* **1999**, *1(10)*, 1575-1578.

23. Belfield, K. D.; Schafer, K.; Mourad, W.; Reinhardt, B. Synthesis of new two-photon absorbing fluorene derivatives via Cu-mediated Ullmann condensations. *J. Org. Chem.* **2000**, *65(15)*, 4475-4481.

24. Pogue, B. W.; Hasan, T. Targeting in photodynamic therapy and photo-imaging. *Optics & Photonics News* **2003**, 37-43.

25. Belfield, K. D.; Schafer, K.. A new photosensitive polymeric material for WORM optical data storage using multichannel two-photon fluorescence readout. *Chem. Mater.* **2002**, *14*, 3656-3662.

26. Belfield, K. D.; Bondar, M.V.; Przhonska, O. V.; Schafer, K.; Mourad, W. Spectral properties of several fluorene derivatives with potential as two-photon fluorescent dyes. *J. Luminescence* **2002**, *97(2)*, 141-146.

27. Kraljic, I. Detection of singlet oxygen and its role in dye-sensitized photooxidation in aqueous and micellar solutions. *Biochimie* **1986**, *68*, 807-811.

28. Gorman, A. A.; Hamblett, I.; Lambert, C.; Prescott, A. L.; Rodgers, M.; Spence, H. M. Aromatic ketone-naphthalene systems as absolute standards for the triplet-sensitized formation of singlet oxygen, in organic and aqueous media: A time-resolved luminescence study. *J. Am. Chem. Soc.* **1987**, *109*, 3091-3097.

29. Krasnovsky, A. A. Singlet molecular oxygen in photobiochemical systems: IR phosphorescence studies. *Membr. Cell Biol.* **1998**, *12(5)*, 665-690.

30. Niedre, M.; Patterson, M. S.; Wilson, B. C. Direct near-infrared luminescence detection of singlet oxygen generated by photodynamic therapy in cell *in vitro* and tissues *in vivo*. *Photochem. Photobiol.* **2002**, *75(4)*, 382-391.

31. Texier, I.; Berberan-Santos, M.; Fedorov, A.; Brettreich, M.; Schonberger, H.; Hirsch, A.; Leach, S.; Bensasson, R. V. Photophysics and photochemistry of water-soluble C_{60} dendrimer: Fluorescence quenching by halides and photoinduced oxidation of I^-. *J. Phys. Chem. A.* **2001**, *105*, 10278-10285.

32. Alegria, A. E.; Ferrer, A.; Santiago, G.; Sepulveda, E.; Flores, W. Photochemistry of water-soluble quinones. Production of the hydroxyl radical singlet oxygen and the superoxide ion. *J. Photochem. Photobiol. A: Chemistry* **1999**, *127*, 57-65.

33. Tanielian, C.; Heinrich, G. Effect of aggregation on the hematoporphyrin-sensitized production of singlet molecular oxygen. *Photochem. Photobiol.* **1995**, *61(2)*, 131-135.

34. Tanielian, C.; Wolff, C. Determination of the parameters controlling singlet oxygen production via oxygen and heavy-atom enhancement of triplet yields. *J. Phys. Chem.* **1995**, *99*, 9831-9837.

35. Ogilby, P. R.; Foote, C. S. Chemistry of singlet oxygen. Unexpected solvent deuterium isotope effects on the lifetime of singlet molecular oxygen. *J. Am. Chem. Soc.* **1981**, *103*, 1219-1221.

36. Foote, C. S.; Denny, R. W. Chemistry of singlet oxygen. XIII. Solvent effects on the reaction with olefins. *J. Am. Chem. Soc.* **1971**, *93(20)*, 51685171.

37. Kraljic, I.; Sharpatyi, V.A. Determination of singlet oxygen rate constants in aqueous solutions. *Photochem. Photobiol.* **1978**, *28*, 583-586.

38. Merkel, P. B.; Kearns, D. R. Radiationless decay of singlet molecular oxygen in solution. An experimental and theoretical study of electronic-to-vibrational energy transfer. *J. Am. Chem. Soc.* **1972**, *94(21)*, 7244-7253.

39. Lindig, B. A.; Rodgers, M. A. J.; Schaap, P. Determination of lifetime of singlet oxygen in D_2O using 9,10-anthracenedipropionic acid, a water-soluble probe. *J. Am. Chem. Soc.* **1980**, *102*, 5590-5593.

40. Merkel, P. B.; Kearns, D. R. Remarkable solvent effects on the lifetime of $^1\Delta_g$ oxygen. *J. Am. Chem. Soc. Comm.* **1972**, *94(3)*, 1029-1030.

41. Tanielian, C.; Wolff, C.; Esch M. Singlet oxygen production in water: Aggregation and charge-transfer effects. *J. Phys. Chem.* **1996**, *100*, 6555-6560.

42. Schmidt, R.; Tanielian, C.; Dunsbach, R.; Wolff, C. Phenalenone, a universal reference compound for the determination of quantum yields of singlet oxygen O_2 ($^1\Delta_g$) sensitization. *J. Photochem. Photobiol. A: Chem.* **1994**, *79*, 11-17.

43. Nardello, V.; Brault, D.; Chavalle, P.; Aubry, J.M. Measurement of photogenerated singlet oxygen (O_2 ($^1\Delta_g$)) in aqueous solution by specific chemical trapping with sodium 1,3-cyclohezadiene-1,4-diethanoate. *J. Photochem. Photobiol. B: Biology* **1997**, *39*, 146-155.

44. Tanielian, C.; Wolff, C. Porphyrin-sensitized generation of singlet molecular oxygen: Comparison of steady-state and time-resolved methods. *J. Phys. Chem.* **1995**, *99*, 9825-9830.

45. Kuznetsova, N. A.; Gretsova, N.; Yuzhakova, O. A.; Negrimovskii, V. M.; Kaliya, O. L.; Luk'yanets, E. A. New reagents for determination of quantum efficiency of singlet oxygen generation in aqueous media. *Russian J. of Gen. Chem.* **2001**, *71(1)*, 36-41.

46. Murassecco, P.; Oliveros, E.; Braun, A. M.; Monnier, P. Quantum yield measurements of the hematoporphyrin derivative (Hpd) sensitized singlet oxygen production. *Photobiochem. Photobiophys.* **1985**, *9*, 193-201.

47. Spiller, W.; Kliesch, H.; Wohrle, D.; Hackbarth, S.; Roder, B.; Schnurpfeil, G. Singlet oxygen quantum yields of different photosensitizers in polar solvents and micellar solutions. *J. Porph. and Phthal.* **1998**, *2*, 145-158.

48. Amat-Guerri, F.; Lempe, E.; Lissi, E. A.; Rodriguez, F. J.; Trull, F. R. Water-soluble 1,3-diphenylisobenzofuran derivatives. Synthesis and evaluation as singlet molecular oxygen acceptors for biological systems. *J. Photochem. Photobiol. A: Chem.* **1996**, *93*, 49-56.

49. Detty, M. R.; Merkel, P. B. Chalcogenapyrylium dyes as potential photochemotherapeutic agents. Solution studies of heavy atom effects on triplet yields, quantum efficiencies of singlet oxygen generation, rates of reaction with singlet oxygen, and emission quantum yields. *J. Am. Chem. Soc.* **1990**, *112*, 3845-3855.

50. Zecasin, S.A. Photochemical production and quenching of singlet oxygen by the porphyrins used in photodynamic therapy of cancer. *Romanian J. Biophys.* **1996**, *6(3)*, 205-212.

51. Corredor, C. M.S. thesis, University of Central Florida, Orlando, FL, 2003.

52. Kraljic, I.; Mohsni, S. E. A new method for the detection of singlet oxygen in aqueous solutions. *Photochem. Photobiol.* **1978**, *28*, 577-581.

53. Profio, A.E.; Shu, K.H. Measurements of singlet oxygen in photodynamic therapy. *SPIE Vol. 1065 Photodynamic Therapy: Mechanisms* **1989**, 123-127.

54. Kuznetsova, N.A.; Grestova, N; Derkacheva, V.; Mikhalenko, S.; Solov'eva, L.; Yuzhakova, O.; Kaliya, O.; Luk'yanets, E. Generation of singlet oxygen with anionic aluminum phthalocyanines in water. *Russian J. Gen. Chem.* **2002**, *72*, 300-306.

55. Verlhac, J.B.; Gaudemer, A. Water-soluble porphyrins and metalloporphyrins as photosensitizers in aerated aqueous solutions. I. Detection and determination of quantum yield of formation of singlet oxygen. *Nouveau Journal de Chimie*, **1984**, *8*, 401-406.

56. Haag, W. R.; Hoigne, J.; Gassman, E.; Braun, A. M. Singlet oxygen in surface waters-Part I: Furfuryl alcohol as a trapping agent. *Chemosphere* **1984**, *13(5-6)*, 631-640.

57. Braun, A. M.; Dahn, H.; Gassman, E.; Gerothanassis, I.; Jakob, L.; Kateva, N.; Martinez, C.; Oliveros, E. (2+4)-cycloaddition with singlet oxygen. ^{17}O-investigation of the reactivity of furfuryl alcohol endoperoxide. *Photochem. Photobiol.***1999**, *70(5)*, 868-874.

58. Haag, W. R.; Hoigne, J.; Gassman, E.; Braun, A. M. Singlet oxygen in surface waters-Part II: Quantum yields of its production by some natural humic materials as a function of wavelength.

Chemosphere **1984**, *13(5-6)*, 641-650.

59. Shahriari, M.R.; Murtaugh, M.T.; Kwon, H.C. Ormosil Thin Films for Chemical Sensing Platforms. *Chemical, Biochemical and Environmental Fiber Sensors IX*, **1997**, SPIE, 3105, 40-5

60. Krihak, M.; Murtaugh, M.T.; Shahriari, M.R. Fiber Optic Oxygen Sensors Based on the Sol-Gel Coating Technique. *Chemical, Biochemical and Environmental Fiber Sensors VIII*, **1996**, SPIE, Vol. 2836.

61. Wang, W.; Reimers, C.E.; Wainright, S.C.; Shahriari. M.R.; Morris, M.J. Applying Fiber-Optic Sensors for Monitoring Dissolved Oxygen. *Sea Technology* **1999**, *40 (3)*, 69-74.